BEHAVIOR OF GROUTED PILE CONNECTIONS

by

REGINALD VAN LEE

S.B., Massachusetts Institute of Technology
(1979)

SUBMITTED IN PARTIAL FULFILLMENT
OF THE REQUIREMENTS FOR THE
DEGREE OF

MASTER OF SCIENCE
IN CIVIL ENGINEERING

at the

MASSACHUSETTS INSTITUTE OF TECHNOLOGY

June 1980

© Reginald Van Lee   1980

Signature of the Author ....
Department of Civil Engineering
April 10, 1980

Certified by ....
Michael N. Fardis
Thesis Supervisor

Accepted by ....
C. Allin Cornell
Chairman, Department Committee

BEHAVIOR OF GROUTED PILE CONNECTIONS

by

REGINALD VAN LEE

ABSTRACT

The connections between steel offshore platforms and the foundation piles are generally made by filling the annulus between each pile and its sleeve with cement grout. The grouted connection forms the only structural connection between the jacket and the foundation and the grout is required to transmit forces arising both from the dead weight of the jacket, deck and superstructure, and from wave or seismic loading. The strength of axially loaded grouted connections is generally described in terms of an equivalent bond strength which is obtained by dividing the ultimate capacity of the connection by the total surface area of the pile-grout interface.

The objective of this study is to define the principal parameters which affect the behavior of grouted connections and describe the effects of these parameters by means of structural mechanics. Two analytical mechanical models were developed and their capability of predicting the structural behavior of the connection was tested by comparison with experimental results. Two finite element models were developed and tested also.

The results show good agreement of the model which accounts for Poisson effects but ignores bending of the components, with experimental data. The ultimate bond strength of grouted connections depends primarily on the strength and stiffness of the steel-grout interface and on grout strength. Since for typical stiffnesses of the steel-grout interface the distribution of shear stress along the connection is almost uniform, the current practice of describing the ultimate strength of axially loaded grouted connections in terms of an average bond strength seems valid.

The non-linear behavior of the steel-grout interfaces does not appreciably affect the behavior of normal stresses and deformations in the connection and since it has a uniformizing effect on the distribution of shear stress along the connection, it adds validity to the description of the strength of the connection by means of an average bond strength. The actual slippage along the connection in the post-ultimate range can be predicted only be a non-linear finite element analysis.

Thesis Supervisor: Dr. Michael N. Fardis

        Title: Assistant Professor of Civil Engineering

ACKNOWLEDGEMENTS

The particular tasks performed towards the completion of this thesis may have been the work of one person however I could not have successfully accomplished such a goal without the support, guidance and encouragement of several persons to whom I would now like to extend my eternal thanks:

First I would like to thank Prof. Fardis for his undying patience, optimism when situations seemed gloomiest and his genuine interest and concern both in the thesis and in me as a person.

I would like to thank also Mssrs. Joe McGraw and Jim Lloyd of the Exxon Production Research Company in Houston, Texas for assisting me in the choice of this thesis topic and in procuring vital information to the analysis.

My gratitude is also extended to the friends and relatives who have lent encouragement and supportive words to help develop the type of perseverence and determination that I have found essential to coping with student life at M.I.T.

Finally, I would like to thank my parents, Tommie and Eva Elnora Lee, whose love, encouragement and constant sacrafices made my years at M.I.T. as pleasant an experience as they could. My parents have been the guiding forces in my life and to them I am eternally grateful and indebted.

TABLE OF CONTENTS

LIST OF FIGURES

CHAPTER 1: INTRODUCTION

1.1. HISTORICAL OVERVIEW

The most popular form of construction for fixed off-shore platforms is the piled steel jacket. The steel tubular piles are driven through the legs of the structure or through tubular sleeves attached to the lower part of the structure. The annulus between pile and jacket leg or sleeve is then filled with cement grout thus providing a connection which may be additional to or may replace a welded connection. Grouting reduces corrosion of the pile and of the interior surface of the leg, improves the mechanism of load transfer by achieving continuous transfer along the leg and provides some reinforcement to the brace to leg joints.

In shallow water, normally a single pile is placed through each leg of the structure and often extends to the top of the leg so that the deck structure is welded directly to the pile. The jacket resists the effects of wave loading, stabilizes the piles and stiffens the complete structure whereas the grout transmits lateral forces between the piles and the jacket but is not normally required to transmit vertical loads from the deck super-structure to the piles. Bond stresses at the interfaces between steel and grout are low and debonding is unlikely to have an effect on overall structural stability.

In deeper water, however, the piles do not extend to the surface and are either grouted in clusters around the main legs of the structure or in some cases are evenly distributed around the base of the structure. The grouted connection forms the only structural connection between the jacket and its foundations and the grout is required to transmit forces arising both from the dead weight of the jacket, deck and superstructure, and from wave, current or seismic loading. In addition, with the development of offshore oil fields in deeper water, the capacity of offshore construction facilities for handling and driving piles has increased, resulting in a trend towards foundations consisting of smaller numbers of large diameter and less radially stiff connections. In view of the increasing importance of grouted connections and of the trend towards larger diameters, a large research effort has been directed into defining the principal parameters which affect the strength of grouted connections and establishing design procedures which describe the effects of these parameters.

1.2 THE PROBLEM

The strength of axially loaded grouted connections is generally described in terms of an equivalent bond strength which is obtained by dividing the ultimate capacity of the connection by the total surface area of the

interface between the pile and the grout. For identical grouts the bond strength actually attained in the annulus between two steel pipes can vary as much as threefold due to independent factors and conditions. Experimental data also have shown that with identical design and conditions, two grouts with the same compressive strength but different expansion properties can show bond strengths which differ as much as fivefold.

Final shear bond strength depends on a combination of independent factors and grout properties. Those independent factors include interface surface condition or modification, confinement potential or radial stiffness and moisture environment or access to external water. The relevant grout properties are expansion potential, compressive or shear strength, corrosion at bond interface and chemical or adhesive bond due to special admixtures. Shear bond strength in a steel annulus is far from an intrinsic property of the hardened grout. However when all independent factors, corrosion at bond interface and chemical or adhesive bond are the same, shear bond strength depends mainly on compressive strength.

Several attempts have been made to correlate bond strengths to compressive strengths using equations of the form:

$$f_b = A f_{cu}^{0.5}$$

where f_b is the ultimate bond strength, f_{cu} is the grout cube strength, A is a factor which depends upon surface roughness and geometry of the pile and the sleeve. Generally, the rougher the steel surface the higher the shear bond strength. However, a reliable correlation between roughness and bond strength has not been developed.

Confinement potential is sometimes referred to as radial stiffness factor. Several equations have been proposed for the radial stiffness factor and most appear to have some validity. They serve three principal purposes: (1) they provide a means to predict actual bond strength from a test model which is not a true scale model of the jacket-pile system, (2) they reveal certain parameters which can be useful in the design of the jacket-pile connection, and (3) they provide a method for comparing grout performance data from different test models. If the radial stiffness of the complete connection is considered, various stiffness factors proportional to the radial stiffness of pile, sleeve and grout cylinders can be derived depending on assumptions regarding the distribution of forces in the grout and the compatibility of displacements or forces across the interfaces between steel and grout.

Thus far little progress has been made towards the determination of actual shear bond stress as a function of position along tubular member. At present an average

shear stress value is employed, obtained by dividing the ultimate capacity of the connection by the total surface area of the pile-grout interface. The use of an average shear stress to describe the behavior, or predict the strength of grouted connections is questionable. It therefore becomes important to formulate a mathematical model which describes the shear stress along the length of the tubular member.

1.3. REVIEW OF PREVIOUS RESEARCH EFFORTS

Heretofore, most studies concerning the bond strength of offshore platform grouts have been purely experimental. Attempts to correlate empirical data to structural theory are limited. The most extensive studies have investigated the effects of grout properties, surface condition of the steel, radial stiffness and length to diameter of the test specimen on the bond strength.

Testing at full scale requires very high testing capacities to reach ultimate load for even relatively short specimens. However, reduced scale modelling techniques have been developed which give results in terms of bond strengths directly comparable with those from full scale tests.

The relationship between bond strength and grout compressive strength has been derived from reduced scale test data. Equations such as that given in Section 1.2.,

$f_b = A f_{cu}^{0.5}$, represent a least squares fit to ultimate bond strengths obtained from test results. Bond strength is not a linear function of compressive strength, (Ostroot, 1978), and this is evident from such an equation.

Variations in surface roughness have a dramatic effect on bond strength. The effect of epoxy coating on the pile is to reduce the bond strength from that of the shot blasted condition significantly. Similar results have been obtained when the surface roughness is reduced by grinding the steel surface demonstrating that the reduction in bond is not a chemical bonding effect. A reliable roughness factor to predict changes in bond strength from changes in roughness has not been developed. (Billington and Gael, 1978)

Forming a chemical or adhesive bond to the steel by adding admixtures such as latex to the grout has potential for increasing the bond strength, but unless extra mixing water is used such admixtures cause large increases in grout viscosity. The extra water needed to prevent mixing and placement problems often causes enough compressive strength loss to offset any advantage for increased bond strength. (Ostroot, 1978)

The effects of radial stiffness of the connection have been studied and results show that the ultimate bond strength is extremely sensitive to specimen geometry and is dependent on the radial stiffness of the sleeve, pile

and grout. (Billington and Gael, 1978) If the radial stiffness of the complete connection is considered, various stiffness factors proportional to the radial stiffness of the pile, sleeve and grout cylinders can be derived.

One of the first stiffness factors devised could be defined as an inverse confinement modulus without a jacket-pile-material constant and was an empirical correlation based on bond strength test results. In a dimensionless form this correlation is:

$$SF = (D_s^2/t_g)(1/t_g + 1/t_p)$$

where D_s = inner diameter of jacket

t_g = grout thickness

t_s = jacket wall thickness

t_p = pile wall thickness

Experimental results with expansive grouts show that when this stiffness factor increases bond strength decreases. (Ostroot, 1978)

A more recently proposed stiffness factor referred to as K is:

$$K = S_g + (1/S_p + 1/S_s)^{-1}, \text{ force/unit area}$$

where $S = E\, t/d$ and g denotes the grout, p the pile, s the sleeve (jacket) and E = Young's modulus.

Claims have been made that f_b is a linear function of K with the general equation being $f_b = BKf_{cu}^{0.5}$ where B depends upon the length to diameter ratio of the connection and on the surface roughness. (Billington and Gael,

1978) This claim has not been completely supported by
data. (Ostroot, 1978)

1.4. OVERVIEW OF THE THESIS

Three mathematical models of the connection are pre-
sented here: The first two are analytical models which
consider linear, elastic isotropic behavior and neglects
any bending of the components. One is an axisymmetric
model which takes into account the radial geometry, but
considers only longitudinal normal stresses (i.e. in
the direction of the tubular members) and shear stresses;
the second, is an axisymmetric model which additionally
accounts for all normal stresses (including radial and
circumferential). The third model is a finite element
axisymmetric model which considers the steel and the
grout as linear elastic but accounts for the non-linear
relationship between bond shear stress and deformation
or slip at the steel-grout interfaces as well as bending
of the components. The results of these models are com-
pared among themselves and to experimental results from
a test model representing a typical design.

These results show that although the one-dimensional
model gives a good approximation to the actual behavior,
the three-dimensional and the finite element models are
by far superior, since they account also for the radial
and hoop stresses and strains. These effects can be very

significant. Bending effects appear negligible to the overall behavior and therefore the finite element model and the three-dimensional model are in good agreement. The three-dimensional model adequately predicts the behavior of the structural system in the linear range of the bond stress-slip relationship.

Results also show that we can describe the strength of the connection in terms of an equivalent average bond strength since the actual distribution of shear stress along the connection is almost uniform. The non-linear behavior of the steel-grout interfaces does not alter appreciably the behavior of normal stresses and deformations but alters slightly the behavior of the shear stress at those interfaces, however the distribution of stress along the connection remains nearly constant.

Although the three-dimensional and linear finite element models give a good approximation to the actual distributions of stresses in the connection even in the plastic range, the inelastic finite element model is the only one that can predict the actual slippage along the connection in this latter range.

Full scale testing to failure requires very high load capacities for even relatively short specimens. However, reduced scale modelling techniques have been developed giving results in terms of bond strengths which are then extrapolated to full scale.

1.5. THE TEST MODEL

Grouted connection tests performed by the Chicago Bridge and Iron Company provide the experimental model used to validate the three mathematical models developed. A series of tests on pile connection models was performed on specimens approximately one-quarter scale. The specimens consisted of an 8 in. (inner) diameter inner cylinder representing the pile and a 12 in. (inner) diameter outer cylinder representing the structure. The surfaces of the cylinders were smooth and the annular space between them was filled from the top with grout. A typical test arrangement is shown in Figure 1.1. below:
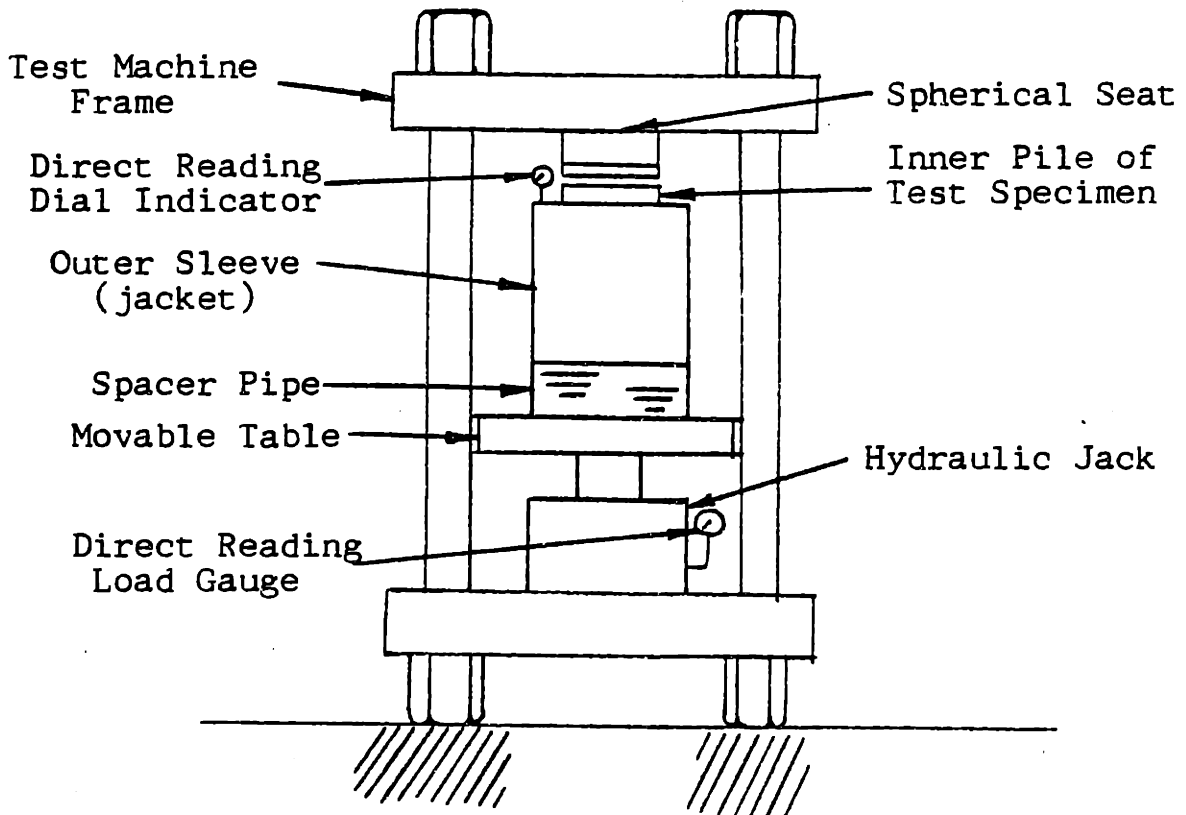
Figure 1.1. Test Arrangement for Bond Tests

The specimens were tested in a specially constructed test frame which applied a downward load on the inner cylinder and an opposite load on the outer. An incremental loading scheme was used and the amount of relative movement between the upper ends of the two pipes was measured with a dial indicator for each increment of load. An average bond stress between the grout and pile surface was calculated by dividing the load by the contact area between the grout and the pile surface.

The thicknesses of both the jacket and the pile steel cylinders were 0.3125 in., that of the grout layer was 1.6875 in., the bonded length was 19.5 in. and the bond area on the pile was approximately 530 square inches.

Typical results of these tests are given in Figure 1.2. in the form of a plot of average bond stress (in psi) versus deformation or slip (in inches). This graph served as the prototype for the mathematical models developed.
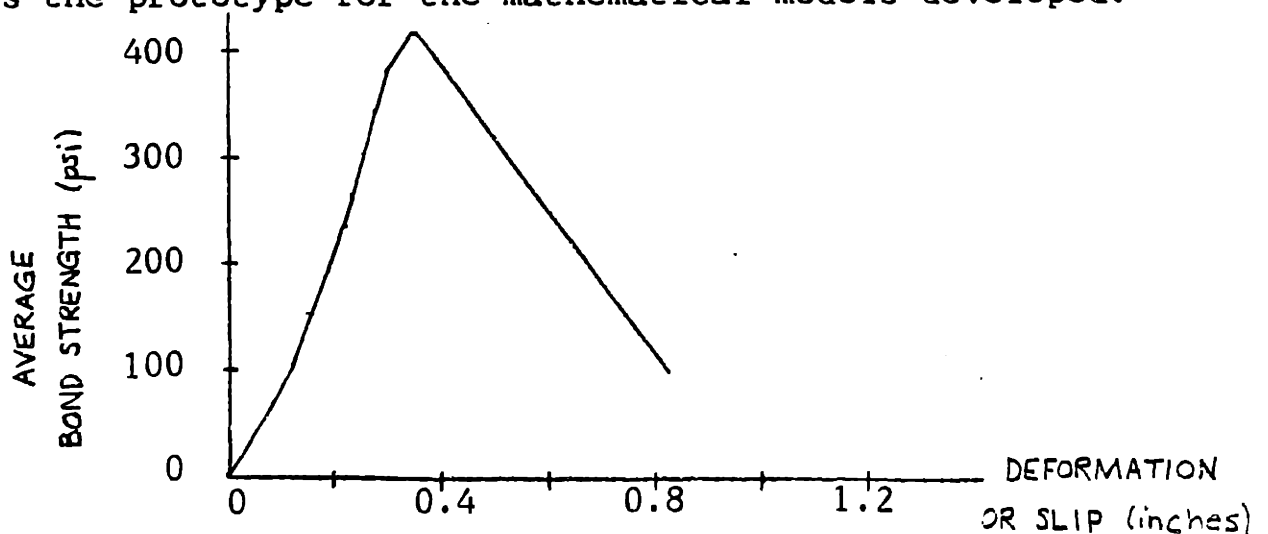
Figure 1.2. Axial Load Failure Tests on One-Quarter Scale Model

CHAPTER 2: BOND STRESS-SLIP RELATIONSHIP OF STEEL--GROUT INTERFACE

The steel-grout interface is the most important component of the connection system. However, modelling of the interface is difficult due to the lack of reliable information on the local bond stress-slip relationship. Experimental data from steel bar pullout tests in concrete are available and provide a relationship between local bond stress and corresponding slip or deformation, however such data exist only for deformed reinforced bar specimens. The experimental data on smooth steel surfaces which provide shear versus deformation relationships are based on gross average shear stress and do not refer to local bond stress and slip. Figure 2.1. presents a representative bond stress-slip curve for deformed reinforced bars.
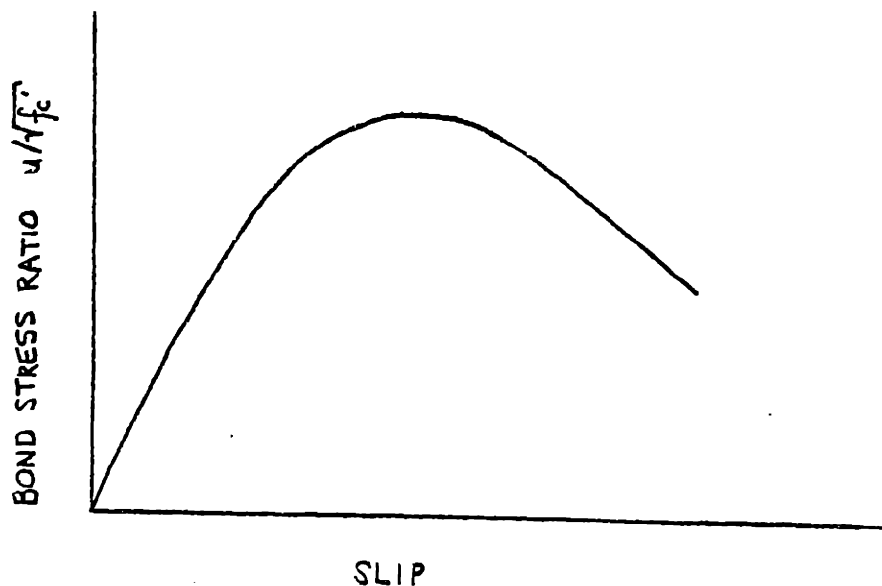
Figure 2.1. Bond Stress-Slip Curve
for Deformed Reinforced Bars

The values from such a graph are not applicable to
the case of a smooth steel surface, however they do express
the general trend of stress vs. deformation for such a
case. It was therefore necessary to combine information
on local bond stress-slip for deformed bars with data on
gross average shear stress versus deformation for smooth
steel surfaces in order to arrive at the interface stiff-
ness employed in this analysis.

The local bond stress versus slip relationship used
in this study is shown in Figure 2.2.

The value of k used
in the analysis was
k = 21000.0 psi/in.
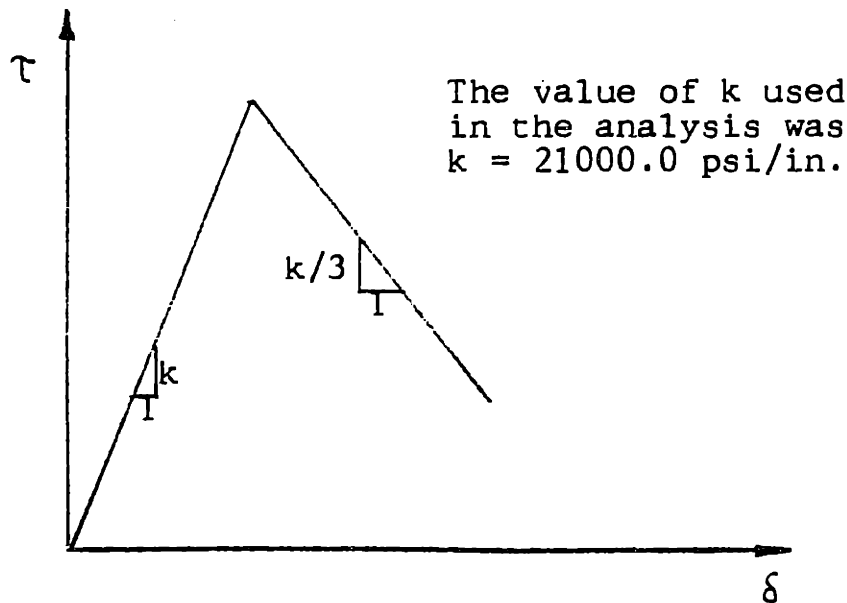
Figure 2.2. Local Bond Stress versus Slip
Relationship

Notice that because of its frictional nature, a real-
istic relationship between τ and δ must include the nor-
mal stress σ as a parameter also. However, because of
the unavailability of data this effect is not included

in the analysis. Since the three-dimensional and the finite element models give radial stresses normal to the interfaces, these models can be supplemented in the future to include the effect of σ on the τ-δ relationship.

For the purposes of the analysis, the following grout properties were assumed: Young's Modulus for the grout was assumed to be 2.92×10^6 psi, Poisson's ratio for the grout was 0.17 and the Shear Modulus for the grout was 1.25×10^6 psi.

CHAPTER 3: ANALYTICAL MODELS

Two analytical models were developed: both models
are linear, elastic and account for cylindrical geometry
and the local deformations (slip) along the steel-grout
interfaces but neglect bending of the pile, the sleeve
or the grout. The first model, called here "one-dimen-
sional" neglects all normal stresses except those in the
longitudinal direction. The second model called here
"three-dimensional" includes all three normal stress com-
ponents and thereby accounts for the Poisson effects.
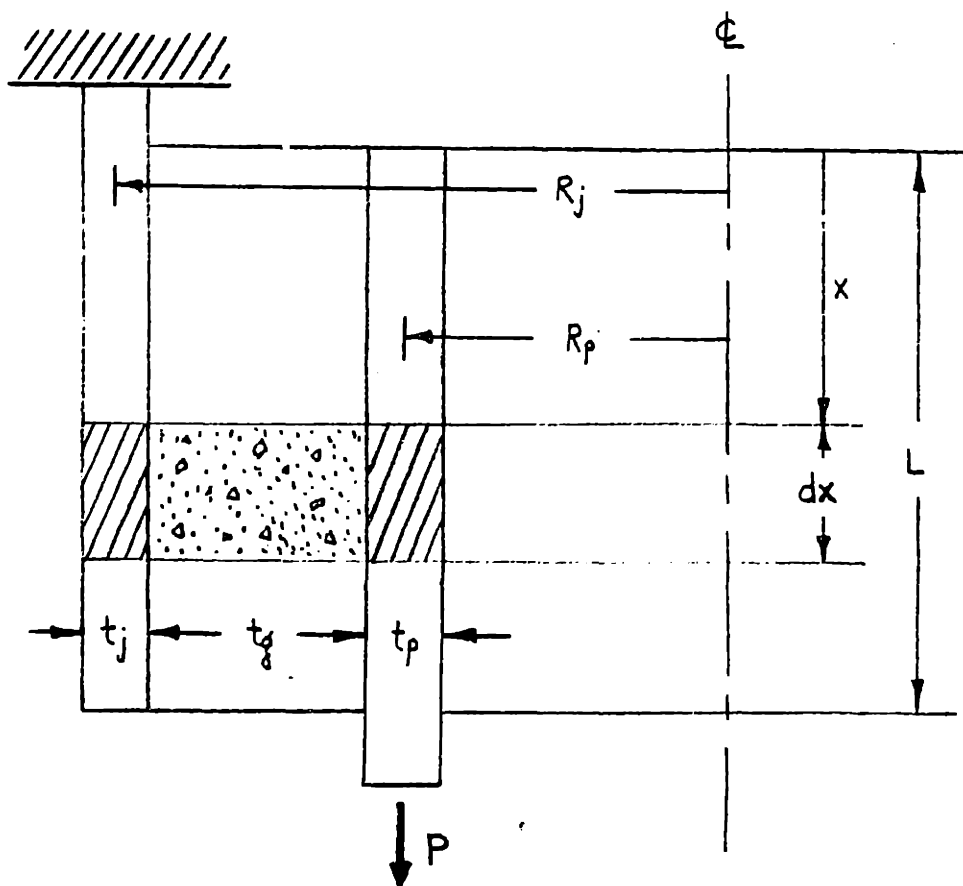
The geometry of both models appears in Figure 3.1.

Figure 3.1. Geometry of Analytical Models
of the Grouted Pile Connection

where t_j = thickness of jacket

t_p = thickness of pile

t_g = thickness of grout

R_j = radius of jacket cylinder

R_p = radius of pile cylinder

P = Axial load

L = Length of connection

x = Axial coordinate along the connection

3.1. ONE-DIMENSIONAL AXISYMMETRIC LINEAR MODEL

The method of solution employed in this model uses the stress equilibrium equations, the normal stress-strain relations, shear stress-strain relations, the strain-displacement equations and the geometric compatibility equations in the three material layers. The combination thereof produced a fourth order differential equation. By setting appropriate boundary conditions on the normal stresses in the jacket and the pile, a solution was obtained.

Some additional notation is introduced:

G_g = Shear Modulus for grout

E_j = Young's Modulus for jacket steel

E_p = Young's Modulus for pile steel

E_g = Young's Modulus for grout

In addition to linearity and elasticity, the assumptions employed by the first model are the following:

1) Only axial normal stresses (i.e. in the x-direction) are considered. These stresses are denoted by:

σ_j^x = Normal stress in jacket in x-direction

σ_p^x = Normal stress in pile in x-direction

σ_g^x = Normal stress in grout in x-direction

and are assumed constant throughout the thickness of the corresponding component (i.e. they depend only on x and bending is neglected).

2) Shear stresses vary linearly through the thickness of each component. Because there are no shear stresses on the inner surface of the pile and on the outer surface of the sleeve, the distribution of shear stresses through the system at given x is as in the figure below, Figure 3.2, with the shear stress at the jacket-grout interface denoted by τ_j and with that at the pile-grout interface denoted by τ_p.
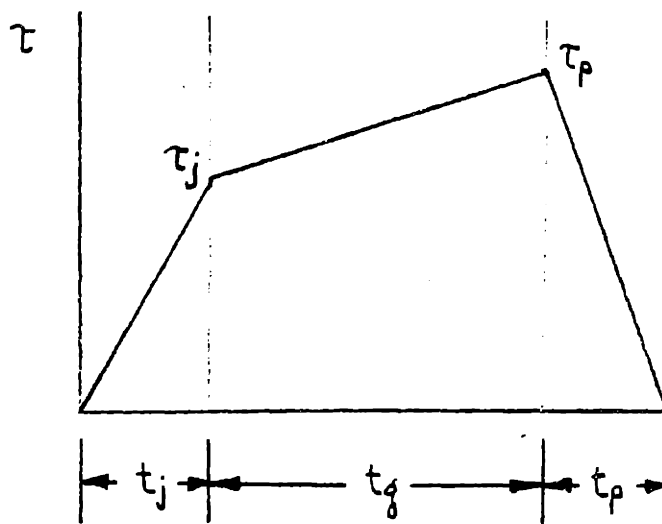
Figure 3.2. Assumed Distribution of Shear Stress Through the System

3)   Shear deformations in the steel components are neglected, implying that the axial displacements in these components,

$u_j{}^x$ = Displacement in jacket in x-direction

$u_p{}^x$ = Displacement in pile in x-direction

$u_g{}^x$ = Displacement in grout in x-direction

depend on x alone.

Equilibrium

Satisfying force equilibrium in the jacket and pile steel layers, one obtains the following force block diagrams and static equilibrium equations --

JACKET:

$$\therefore \left\{ (R_j - t_j/2)\,\tau_j = R_j t_j \frac{\partial \sigma_j{}^x}{\partial x} \right\} \quad (1)$$

PILE:

$$\therefore \left\{ -(R_p + t_p/2)\,\tau_p = R_p t_p \frac{\partial \sigma_p{}^x}{\partial x} \right\} \quad (5)$$
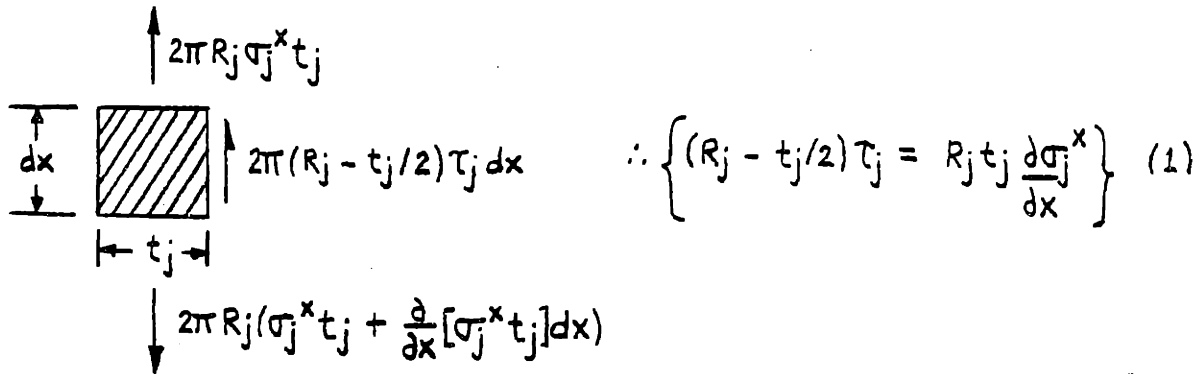
Since τ varies linearly from τ_j to τ_p through the

grout, force equilbrium in the grout layer gives --

GROUT:

$$2\pi\left(R_p + \frac{t_p+t_g}{2}\right)\sigma_g{}^x t_g$$

$$2\pi(R_j - t_j/2)\tau_j\,dx \qquad 2\pi(R_p + t_p/2)\tau_p\,dx$$

$$2\pi\left(R_p + \frac{t_p+t_g}{2}\right)\left[\sigma_g{}^x t_g + \frac{\partial}{\partial x}(\sigma_g{}^x t_g)dx\right]$$

$$\therefore \left\{(R_p + t_p/2)\tau_p - (R_j - t_j/2)\tau_j = \frac{d\sigma_g{}^x}{dx}t_g\left(R_p + \frac{t_p+t_g}{2}\right)\right\} \quad (3)$$

Normal stress-displacement relationships

JACKET: $\left\{\dfrac{\partial u_j{}^x}{\partial x} = \dfrac{\sigma_j{}^x}{E_j}\right\}$ (7)
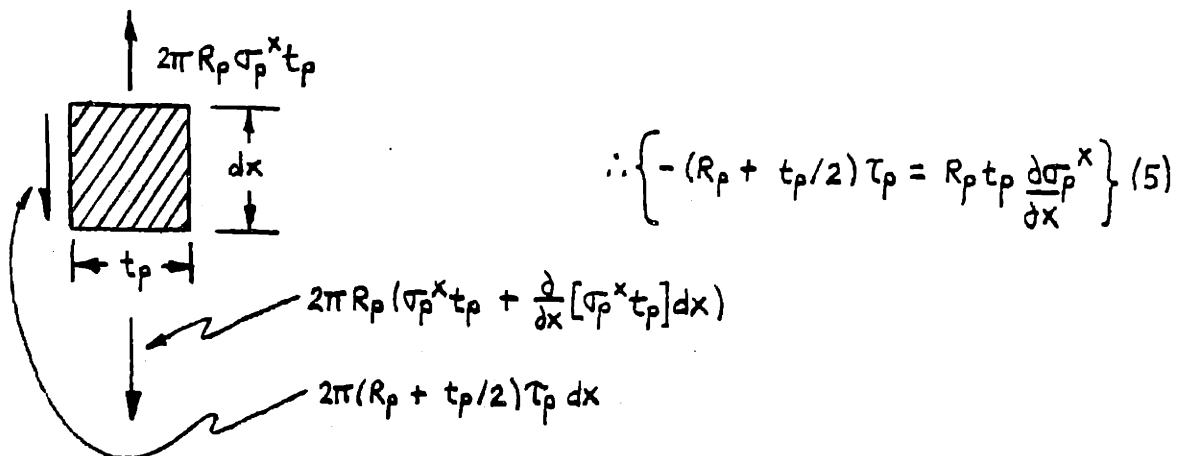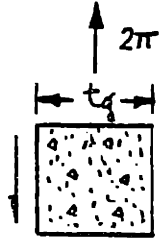
PILE: $\left\{\dfrac{\partial u_p{}^x}{\partial x} = \dfrac{\sigma_p{}^x}{E_p}\right\}$ (9)

Consistent with the assumption that τ varies linear-

ly from τ_j to τ_p through the grout, and since the shear

flexibility of the grout is included the axial displace-

ments in the grout vary quadratically. Due to slippage

at the jacket-grout and pile-grout interfaces, one must

define four (4) displacements at those interfaces as shown

in Figure 3.3. The displacements through the grout vary

quadratically as shown in Figure 3.4.

Since $\sigma_g{}^x$ is considered constant through the thickness

of the grout we use the average value of $u_g{}^x$ in the stress
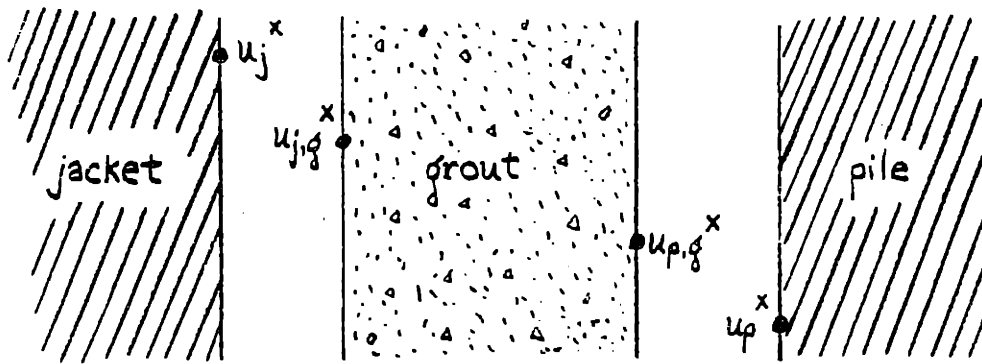
Figure 3.3. Four Longitudinal Displacements at the Interface
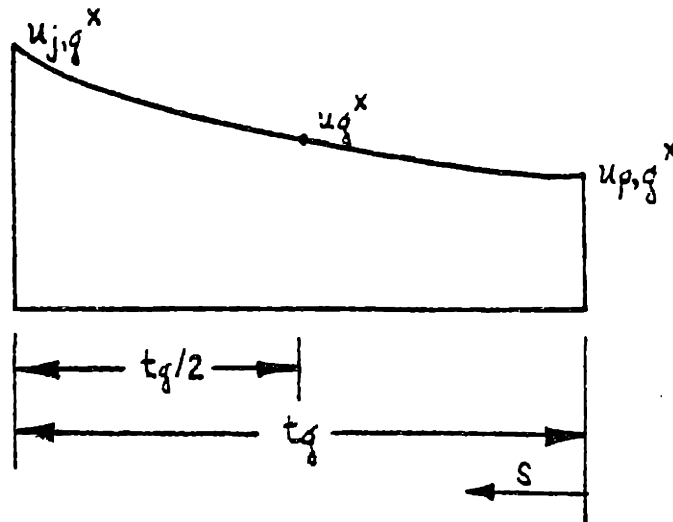
Figure 3.4. Quadratic Behavior of Longitudinal Displacements Through The Grout

displacement relation in the grout. This average is equal to: $\bar{u}_g{}^x = \dfrac{u_{j,g}{}^x + 4u_g{}^x + u_{p,g}{}^x}{6}$. Therefore,

$$\left\{ \frac{\sigma_g{}^x}{E_g} = \frac{\partial}{\partial x}\left(\frac{u_{j,g}{}^x + 4u_g{}^x + u_{p,g}{}^x}{6} \right) \right\} \quad (11)$$

Shear stress-displacement relationships in the grout

Remembering that τ varies linearly from τ_j to τ_p

through the grout --

$$u_g{}^x = u_{p,g}{}^x + \frac{1}{G_g}\int_0^{t_g/2} \tau(s)\,ds = u_{p,g}{}^x + \frac{t_g}{2G_g}\left(\frac{\tau_p}{2} + \frac{\tau_p + \tau_j}{4}\right)$$

i.e. $\quad \left\{ u_g{}^x - u_{p,g}{}^x = \frac{t_g}{G_g}\left(\frac{3\tau_p + \tau_j}{8}\right)\right\}$ (15)

Also $\quad u_{j,g}{}^x = u_{p,g}{}^x + \frac{1}{G_g}\int_0^{t_g}\tau(s)\,ds = u_{p,g}{}^x + \frac{t_g}{G_g}\left(\frac{\tau_j + \tau_p}{2}\right)$

i.e. $\quad \left\{ \left(u_{j,g}{}^x - u_{p,g}{}^x\right) = \frac{t_g}{G_g}\left(\frac{\tau_j + \tau_p}{2}\right)\right\}$ (16)

Shear stress-slip relationship at the interface

To take into account the slippage at the interfaces, let the stiffness derived from the bond stress-slip curve be denoted by K, and write:

$$\left\{ u_j{}^x = u_{j,g}{}^x + \tau_j/K\right\} \quad (17)$$

$$\left\{ u_p{}^x = u_{p,g}{}^x - \tau_j/K\right\} \quad (18)$$

Mathematical Solution

Substituting equations (16) and (15) into equation (11) one finds that $\dfrac{\sigma_g{}^x}{E_g} = \dfrac{1}{6}\dfrac{\partial}{\partial x}\left(6u_{p,g}{}^x + \dfrac{t_p\tau_j}{G_g} + \dfrac{2t_g\tau_p}{G_g}\right)$

Eliminating $u_{p,g}{}^x$, one substitutes equation (18) into the above expression and next replaces $u_p{}^x$ using equation (9) to arrive at $\left\{\dfrac{\sigma_g{}^x}{E_g} = \dfrac{\sigma_p{}^x}{E_p} + \dfrac{1}{K}\dfrac{\partial\tau_p}{\partial x} + \dfrac{t_g}{G_g}\dfrac{\partial}{\partial x}\left(\dfrac{\tau_j + 2\tau_p}{6}\right)\right\}$ (ia)

Differentiating equation (16) and substituting in equations (17), (7), (18) and (9) one obtains --

$$\left\{\frac{\sigma_j{}^x}{E_j} - \frac{1}{K}\frac{\partial\tau_j}{\partial x} = \frac{\sigma_p{}^x}{E_p} + \frac{1}{K}\frac{\partial\tau_p}{\partial x} + \frac{t_g}{G_g}\frac{\partial}{\partial x}\left(\frac{\tau_j + \tau_p}{2}\right)\right\} \quad (iia)$$

Adding equations (1), (3) and (5) and integrating, one

gets -- $\left\{ R_j t_j \sigma_j^x + \left(R_p + \dfrac{t_p + t_g}{2} \right) t_g \sigma_g^x + R_p t_p \sigma_p^x = \dfrac{P}{2\pi} \right\}$ (21)

Substituting T_j and T_p from equations (1) and (5)

respectively into equations (ia) and (iia) respectively

one finds that --

$$\left\{ \frac{\sigma_g^x}{E_g} = \frac{\sigma_p^x}{E_p} + \frac{t_g}{6G_g} \frac{\partial}{\partial x} \left[\left(\frac{2R_j t_j}{2R_j - t_j} \right) \frac{\partial \sigma_j^x}{\partial x} - \left(\frac{4R_p t_p}{2R_p + t_p} \right) \frac{\partial \sigma_p^x}{\partial x} \right] - \frac{1}{K} \frac{\partial}{\partial x} \left[\frac{2R_p t_p}{2R_p + t_p} \right] \frac{\partial \sigma_p^x}{\partial x} \right\}$$ (ib)

and $\left\{ \dfrac{\sigma_j^x}{E_j} = \dfrac{\sigma_p^x}{E_p} + \dfrac{t_g}{2G_g} \dfrac{\partial}{\partial x} \left[\left(\dfrac{2R_j t_j}{2R_j - t_j} \right) \dfrac{\partial \sigma_j^x}{\partial x} - \left(\dfrac{2R_p t_p}{2R_p + t_p} \right) \dfrac{\partial \sigma_p^x}{\partial x} \right] \right.$

$$\left. + \frac{1}{K} \frac{\partial}{\partial x} \left[\frac{2R_j t_j}{2R_j - t_j} \right] \frac{\partial \sigma_j^x}{\partial x} - \frac{1}{K} \frac{\partial}{\partial x} \left[\frac{2R_p t_p}{2R_p + t_p} \right] \frac{\partial \sigma_p^x}{\partial x} \right\}$$ (iib)

Substituting σ_g^x from equation (21) into equation

(ib) -- $\left\{ \dfrac{P}{\pi E_g (2R_p + t_p + t_g) t_g} - \dfrac{2R_j t_j \sigma_j^x}{E_g (2R_p + t_p + t_g) t_g} - \left(\dfrac{2R_p t_p}{E_g (2R_p + t_p + t_g) t_g} + \dfrac{1}{E_p} \right) \sigma_p^x \right.$

$$\left. = \frac{R_j t_j t_g}{3G_g (2R_j - t_j)} \frac{\partial^2 \sigma_j^x}{\partial x^2} - \frac{2R_p t_p t_g}{3G_g (2R_p + t_p)} \frac{\partial^2 \sigma_p^x}{\partial x^2} - \frac{2R_p t_p}{K(2R_p + t_p)} \frac{\partial^2 \sigma_p^x}{\partial x^2} \right\}$$ (ic)

Solving for $\dfrac{\partial^2 \sigma_p^x}{\partial x^2}$ from equation (iib) --

$$\left\{ \frac{\partial^2 \sigma_p^x}{\partial x^2} = \left(-\frac{\sigma_j^x}{E_j} + \frac{\sigma_p^x}{E_p} + \left[\frac{R_j t_j}{2R_j - t_j} \right] \left[\frac{t_g}{G_g} + \frac{2}{K} \right] \frac{\partial^2 \sigma_j^x}{\partial x^2} \right) \left(\left[\frac{2R_p + t_p}{R_p t_p} \right] \left[\frac{K G_g}{K t_g + 2G_g} \right] \right) \right\}$$ (iic)

Substituting into equation (ic) this expression for

$\dfrac{\partial^2 \sigma_p^x}{\partial x^2}$ one gets -- $\left\{ \dfrac{R_j t_j}{2R_j - t_j} \left[\left(\dfrac{t_g}{G_g} + \dfrac{2}{K} \right) \left(\dfrac{2K t_g + 6G_g}{3[K t_g + 2G_g]} \right) - \dfrac{t_g}{3G_g} \right] \dfrac{\partial^2 \sigma_j^x}{\partial x^2} = \dfrac{-P}{\pi E_g t_g (2R_p + t_p + t_g)} \right.$

$$+ \left[\frac{2R_j t_j}{E_g t_g (2R_p + t_p + t_g)} + \frac{(2K t_g + 6G_g)}{3E_j (K t_g + 2G_g)} \right] \sigma_j^x$$

$$\left. + \left[\frac{2R_p t_p}{E_g t_g (2R_p + t_p + t_g)} + \frac{1}{E_p} - \frac{(2K t_g + 6G_g)}{3E_p (K t_g + 2G_g)} \right] \sigma_p^x \right\}$$ (id)

Similarly, solve for $\dfrac{\partial^2 \sigma_j^x}{\partial x^2}$ from equation (ic) and sub-

stitute into equation (iib) and get --

$$\left\{ \frac{R_p t_p}{2R_p + t_p} \left[-\left(\frac{t_g}{G_g} + \frac{2}{K} \right) + \left(\frac{2t_g}{3G_g} + \frac{2}{K} \right) \left(3 + \frac{6G_g}{K t_g} \right) \right] \frac{\partial^2 \sigma_p^x}{\partial x^2} = \frac{-\left(3 + \frac{6G_g}{K t_g} \right) P}{\pi E_g t_g (2R_p + t_p + t_g)} \right. + (cont'd)$$

$$+\left[\frac{R_jt_j\left(6+\frac{12G_q}{kt_q}\right)}{E_qt_q(2R_p+t_p+t_q)}+\frac{1}{E_j}\right]\sigma_j^x+\left[\left(3+\frac{6G_q}{kt_q}\right)\left(\frac{2R_pt_p}{E_qt_q(2R_p+t_p+t_q)}+\frac{1}{E_p}\right)-\frac{1}{E_p}\right]\sigma_p^x\right\}\quad(iid)$$

Differentiate equation (id) twice and get --

$$\left\{\frac{R_jt_j}{2R_j-t_j}\left[\left(\frac{t_q}{G_q}+\frac{2}{K}\right)\left(\frac{2kt_q+6G_q}{3(kt_q+2G_q)}\right)-\frac{t_q}{3G_q}\right]\frac{\partial^4\sigma_j^x}{\partial x^4}=\left[\frac{2R_jt_j}{E_qt_q(2R_p+t_p+t_q)}+\right.$$

$$\frac{(2kt_q+6G_q)}{3E_j(kt_q+2G_q)}\right]\frac{\partial^2\sigma_j^x}{\partial x^2}+\left[\frac{2R_pt_p}{E_qt_q(2R_p+t_p+t_q)}+\frac{1}{E_p}-\frac{(2kt_q+6G_q)}{3E_p(kt_q+2G_q)}\right]\frac{\partial^2\sigma_p^x}{\partial x^2}\quad(ie)$$

Solve for $\frac{\partial^2\sigma_p^x}{\partial x^2}$ from equation (iid) and substitute

this expression into equation (ie). This gives --

$$\left\{\frac{R_jt_j}{2R_j-t_j}\left[\left(\frac{t_q}{G_q}+\frac{2}{K}\right)\left(\frac{2kt_q+6G_q}{3(kt_q+2G_q)}\right)-\frac{t_q}{3G_q}\right]\frac{\partial^4\sigma_j^x}{\partial x^4}=\left[\frac{2R_jt_j}{E_qt_q(2R_p+t_p+t_q)}\right.\right.$$

$$\left.+\frac{2kt_q+6G_q}{3E_j(kt_q+2G_q)}\right]\frac{\partial^2\sigma_j^x}{\partial x^2}+\left\{\left[\frac{-1}{E_p}+\left(3+\frac{6G_q}{kt_q}\right)\left(\frac{2R_pt_p}{E_qt_q(2R_p+t_p+t_q)}+\frac{1}{E_p}\right)\right]\sigma_p^x\right.$$

$$-\frac{\left(3+\frac{6G_q}{kt_q}\right)P}{\pi E_qt_q(2R_p+t_p+t_q)}+\left[\left(6+\frac{12G_q}{kt_q}\right)\frac{R_jt_j}{E_qt_q(2R_p+t_p+t_q)}+\frac{1}{E_j}\right]\sigma_j^x\right\}\frac{\frac{2R_pt_p}{E_qt_q(2R_p+t_p+t_q)}+\frac{1}{E_p}-\frac{(2kt_q+6G_q)}{3E_p(kt_q+2G_q)}}{\frac{R_pt_p}{2R_p+t_p}\left[-\left(\frac{t_q}{G_q}+\frac{2}{k}\right)+\left(\frac{2t_q}{3G_q}+\frac{2}{k}\right)\left(3+\frac{6G_q}{kt_q}\right)\right]}\right\}\quad(if)$$

Solve for σ_p^x from equation (id) --

$$\sigma_p^x=\frac{1}{\left[\frac{2R_pt_p}{E_qt_q(2R_p+t_p+t_q)}+\frac{1}{E_p}-\frac{(2kt_q+6G_q)}{3E_p(kt_q+2G_q)}\right]}\left\{\frac{P}{\pi E_qt_q(2R_p+t_p+t_q)}\right.$$

$$\left.+\frac{R_jt_j}{2R_j-t_j}\left[\left(\frac{t_q}{G_q}+\frac{2}{k}\right)\left(\frac{2kt_q+6G_q}{3(kt_q+2G_q)}\right)-\frac{t_q}{3G_q}\right]\frac{\partial^2\sigma_j^x}{\partial x^2}-\left[\frac{2R_jt_j}{E_qt_q(2R_p+t_p+t_q)}+\frac{(2kt_q+6G_q)}{3E_j(kt_q+2G_q)}\right]\sigma_j^x\right\}$$

Substitute σ_p^x into equation (if) to arrive at the

governing fourth order differential equation below --

$$\frac{R_jt_j}{2R_j-t_j}\left[\left(\frac{t_q}{G_q}+\frac{2}{k}\right)\left(\frac{2kt_q+6G_q}{3(kt_q+2G_q)}\right)-\frac{t_q}{3G_q}\right]\frac{\partial^4\sigma_j^x}{\partial x^4}-\frac{\partial^2\sigma_j^x}{\partial x^2}\left\{\frac{2R_jt_j}{E_qt_q(2R_p+t_p+t_q)}\right.$$

$$\left.+\frac{(2kt_q+6G_q)}{3E_j(kt_q+2G_q)}+\frac{\frac{R_jt_j}{2R_j-t_j}\left[\frac{-1}{E_p}+\left(3+\frac{6G_q}{kt_q}\right)\left(\frac{2R_pt_p}{E_qt_q(2R_p+t_p+t_q)}+\frac{1}{E_p}\right)\right]}{\frac{R_pt_p}{2R_p+t_p}\left[-\left(\frac{t_q}{G_q}+\frac{2}{k}\right)+\left(\frac{2t_q}{3G_q}+\frac{2}{k}\right)\left(3+\frac{6G_q}{kt_q}\right)\right]}\left[\left(\frac{t_q}{G_q}+\frac{2}{k}\right)\left(\frac{2kt_q+6G_q}{3(kt_q+2G_q)}\right)-\frac{t_q}{3G_q}\right]\right\}$$

(CONT'D)

$$-\sigma_j^x \left\{ \frac{\left[\dfrac{2R_p t_p}{E_g t_g(2R_p+t_p+t_g)} + \dfrac{1}{E_p} - \dfrac{(2Kt_g+6G_g)}{3E_p(Kt_g+2G_g)}\right]\left[\dfrac{\left(6+\dfrac{12G_g}{Kt_g}\right)R_j t_j}{E_g t_g(2R_p+t_p+t_g)} + \dfrac{1}{E_j}\right]}{\dfrac{R_p t_p}{2R_p+t_p}\left[-\left(\dfrac{t_g}{G_g}+\dfrac{2}{K}\right)+\left(\dfrac{2t_g}{3G_g}+\dfrac{2}{K}\right)\left(3+\dfrac{6G_g}{Kt_g}\right)\right]} \right.$$

$$\left. - \frac{\left[\dfrac{-1}{E_p} + \left(3+\dfrac{6G_g}{Kt_g}\right)\left(\dfrac{2R_p t_p}{E_g t_g(2R_p+t_p+t_g)} + \dfrac{1}{E_p}\right)\right]\left[\dfrac{2R_j t_j}{E_g t_g(2R_p+t_p+t_g)} + \dfrac{(2Kt_g+6G_g)}{3E_j(Kt_g+2G_g)}\right]}{\dfrac{R_p t_p}{2R_p+t_p}\left[-\left(\dfrac{t_g}{G_g}+\dfrac{2}{K}\right)+\left(\dfrac{2t_g}{3G_g}+\dfrac{2}{K}\right)\left(3+\dfrac{6G_g}{Kt_g}\right)\right]} \right\}$$

$$= \frac{P\left\{-\left[\dfrac{2R_p t_p}{E_g t_g(2R_p+t_p+t_g)} + \dfrac{1}{E_p} - \dfrac{(2Kt_g+6G_g)}{3E_p(Kt_g+2G_g)}\right]\left(3+\dfrac{6G_g}{Kt_g}\right)\right\}}{\dfrac{R_p t_p}{2R_p+t_p}\left[-\left(\dfrac{t_g}{G_g}+\dfrac{2}{K}\right)+\left(\dfrac{2t_g}{3G_g}+\dfrac{2}{K}\right)\left(3+\dfrac{6G_g}{Kt_g}\right)\right]\pi E_g t_g(2R_p+t_p+t_g)}$$

$$+ \left. \frac{\left[\dfrac{-1}{E_p} + \left(3+\dfrac{6G_g}{Kt_g}\right)\left(\dfrac{2R_p t_p}{E_g t_g(2R_p+t_p+t_g)} + \dfrac{1}{E_p}\right)\right]}{\pi E_g t_g(2R_p+t_p+t_g)} \right\}$$

Let $A \equiv \dfrac{R_j t_j}{2R_j t_j}\left[\left(\dfrac{t_g}{G_g}+\dfrac{2}{K}\right)\left(\dfrac{2Kt_g+6G_g}{3[Kt_g+2G_g]}\right) - \dfrac{t_g}{3G_g}\right]$

$$B \equiv -\left\{\frac{2R_j t_j}{E_g t_g(2R_p+t_p+t_g)} + \frac{(2Kt_g+6G_g)}{3E_j(Kt_g+2G_g)}\right.$$

$$\left. + \frac{\dfrac{R_j t_j(2R_p+t_p)}{R_p t_p(2R_j-t_j)}\left[-\dfrac{1}{E_p} + \left(3+\dfrac{6G_g}{Kt_g}\right)\left(\dfrac{2R_p t_p}{E_g t_g(2R_p+t_p+t_g)}+\dfrac{1}{E_p}\right)\right]\left[\left(\dfrac{t_g}{G_g}+\dfrac{2}{K}\right)\left(\dfrac{2Kt_g+6G_g}{3(Kt_g+2G_g)}-\dfrac{t_g}{3G_g}\right)\right]}{[-(t_g/G_g+2/K)+(2t_g/3G_g+2/K)(3+6G_g/Kt_g)]}\right\}$$

$$C \equiv -\left\{\left[\frac{2R_p t_p}{E_g t_g(2R_p+t_p+t_g)} + \frac{1}{E_p} - \frac{(2Kt_g+6G_g)}{3E_p(Kt_g+2G_g)}\right]\left[\frac{(6+12G_g/Kt_g)R_j t_j}{E_g t_g(2R_p+t_p+t_g)} + \frac{1}{E_j}\right]\right.$$

$$\left. -\left[\frac{-1}{E_p} + \left(3+\frac{6G_g}{Kt_g}\right)\left(\frac{2R_p t_p}{E_g t_g(2R_p+t_p+t_g)}+\frac{1}{E_p}\right)\right]\left[\frac{2R_j t_j}{E_g t_g(2R_p+t_p+t_g)} + \frac{12Kt_g+6G_g}{3E_j(Kt_g+2G_g)}\right]\right\}\bigg/\frac{R_p t_p}{2R_p+t_p}\left[-\left(\frac{t_g}{G_g}+\frac{2}{K}\right)+\left(\frac{2t_g}{3G_g}+\frac{2}{K}\right)\left(3+\frac{6G_g}{Kt_g}\right)\right]$$

$$D \equiv \frac{P\left(3+\dfrac{6G_g}{Kt_g}\right)\left(\dfrac{2Kt_g+6G_g}{3E_p(Kt_g+2G_g)} - \dfrac{1}{E_p}\right)}{\dfrac{R_p t_p}{2R_p+t_p}\left[-\left(\dfrac{t_g}{G_g}+\dfrac{2}{K}\right)+\left(\dfrac{2t_g}{3G_g}+\dfrac{2}{K}\right)\left(3+\dfrac{6G_g}{Kt_g}\right)\right]\pi E_g t_g(2R_p+t_p+t_g)}$$

Therefore, $A\dfrac{\partial^4 \sigma_j^x}{\partial x^4} + B\dfrac{\partial^2 \sigma_j^x}{\partial x^2} + C\sigma_j^x = D$ becomes the

governing equation. The general solution is of the form --

$$\sigma_j^x = Ee^{-\mu_1 x} + Fe^{-\mu_1 (L-x)} + Ge^{-\mu_2 x} + He^{\mu_2 x} + D/C$$

where $\mu_1^2 = \dfrac{-B + \sqrt{B^2 - 4AC}}{2A}$ and $\mu_2^2 = \dfrac{-B - \sqrt{B^2 - 4AC}}{2A}$.

Applying boundary conditions, one obtains:

At $x = 0$, $\sigma_j^x = E + Fe^{-\mu_1 L} + G + H + D/C = \dfrac{P}{2\pi R_j t_j}$

At $x = L$, $\sigma_j^x = Ee^{-\mu_1 L} + F + Ge^{-\mu_2 L} + He^{\mu_2 L} + D/C = 0$

At $x = 0$, $\sigma_p^x = 0$ i.e.

$$A(\mu_1^2 E + \mu_1^2 Fe^{-\mu_1 L} + \mu_2^2 G + \mu_2^2 H) = \dfrac{-P}{\pi E_g t_g (2R_p + t_p + t_g)} + \beta(E + Fe^{-\mu_1 L} + G + H + D/C)$$

where $\beta = \dfrac{2R_j t_j}{E_g t_g (2R_p + t_p + t_g)} + \dfrac{2kt_g + 6G_g}{3E_j (kt_g + 2G_g)}$

Hence, $(A\mu_1^2 - \beta)E + (A\mu_1^2 e^{-\mu_1 L} - \beta e^{-\mu_1 L})F + (A\mu_2^2 - \beta)G$

$$+ (A\mu_2^2 - \beta)H = \dfrac{-P}{\pi E_g t_g (2R_p + t_p + t_g)} + \dfrac{\beta D}{C}$$

At $x = L$, $\sigma_p^x = \dfrac{P}{2\pi R_p t_p}$.

i.e., if $\gamma = \dfrac{2R_p t_p}{E_g t_g (2R_p + t_p + t_g)} + \dfrac{1}{E_p} - \dfrac{(2kt_g + 6G_g)}{3E_p (kt_g + 2G_g)}$

then

$$e^{-\mu_1 L}(A\mu_1^2 - \beta)E + (A\mu_1^2 - \beta)F + e^{-\mu_2 L}(A\mu_2^2 - \beta)G$$

$$+ e^{\mu_2 L}(A\mu_2^2 - \beta)H = \dfrac{-P}{\pi E_g t_g (2R_p + t_p + t_g)} + \dfrac{\beta D}{C} + \dfrac{\gamma P}{2\pi R_p t_p}$$

In matrix notation, the boundary conditions take the following form:

$$
\begin{bmatrix}
1 & e^{-\mu_1 L} & 1 & 1 \\
e^{-\mu_1 L} & 1 & e^{-\mu_2 L} & e^{\mu_2 L} \\
A\mu_1^2 - \beta & e^{-\mu_1 L}(A\mu_1^2 - \beta) & A\mu_2^2 - \beta & A\mu_2^2 - \beta \\
e^{-\mu_1 L}(A\mu_1^2 - \beta) & A\mu_1^2 - \beta & e^{-\mu_2 L}(A\mu_2^2 - \beta) & e^{\mu_2 L}(A\mu_2^2 - \beta)
\end{bmatrix}
\underset{\underset{\sim}{R}}{}
\begin{Bmatrix}
E \\ F \\ G \\ H
\end{Bmatrix}
=
\begin{bmatrix}
\dfrac{P}{2\pi R_j t_j} - \dfrac{D}{C} \\[2mm]
\dfrac{-D}{C} \\[2mm]
\dfrac{-P}{\pi E_g t_g (2R_p + t_p + t_g)} + \dfrac{\beta D}{C} \\[2mm]
\dfrac{-P}{\pi E_g t_g (2R_p + t_p + t_g)} + \dfrac{\beta D}{C} + \dfrac{\gamma P}{2\pi R_p t_p}
\end{bmatrix}
\underset{\underset{\sim}{T}}{}
$$

Therefore the constants E, F, G and H can be obtained as

$$
\begin{Bmatrix}
E \\ F \\ G \\ H
\end{Bmatrix}
= \underset{\sim}{R}^{-1}\,\underset{\sim}{T}
$$

The final solution is:

$$
\sigma_j^x = E e^{-\mu_1 x} + F e^{-\mu_1 (L-x)} + G e^{-\mu_2 x} + H e^{\mu_2 x} + D/C
$$

$$
\sigma_p^x = \frac{1}{\gamma}\left\{ A\left(\mu_1^2 E e^{-\mu_1 x} + \mu_1^2 F e^{-\mu_1 (L-x)} + \mu_2^2 G e^{-\mu_2 x} + \mu_2^2 H e^{\mu_2 x}\right)\right.
$$
$$
\left. + \frac{P}{\pi E_g t_g (2R_p + t_p + t_g)} - \beta \sigma_j^x \right\}
$$

$$
\sigma_g^x = \frac{P}{\pi (2R_p + t_p + t_g) t_g} - \frac{2R_j t_j\, \sigma_j^x}{(2R_p + t_p + t_g) t_g} - \frac{2R_p t_p\, \sigma_p^x}{(2R_p + t_p + t_g) t_g}
$$

$$
\tau_j = \left(\frac{2R_j t_j}{2R_j - t_j}\right)\left(-\mu_1 E e^{-\mu_1 x} + \mu_1 F e^{-\mu_1 (L-x)} - \mu_2 G e^{-\mu_2 x} + \mu_2 H e^{\mu_2 x}\right)
$$

$$\tau_p = \frac{-2R_p t_p}{Y(2R_p + t_p)} \left\{ A(-\mu_1^3 E e^{-\mu_1 x} + \mu_1^3 F e^{-\mu_1(L-x)} - \mu_2^3 G e^{-\mu_2 x} \right.$$

$$+ \mu_2^3 H e^{\mu_2 x}) - \beta(-\mu_1 E e^{-\mu_1 x} + \mu_1 F e^{-\mu_1(L-x)}$$

$$\left. - \mu_2 G e^{-\mu_2 x} + \mu_2 H e^{\mu_2 x}) \right\}$$

$$\tau_g = \frac{\tau_j + \tau_p}{2} \qquad \text{(average shear stress in the grout)}$$

$$u_j{}^x = \frac{1}{E_j} \int_0^x \sigma_j{}^x \, dx = \frac{1}{E_j} \left(\frac{1}{\mu_1} \left[-E e^{-\mu_1 x} + E + F e^{-\mu_1(L-x)} - F e^{-\mu_1 L} \right] \right.$$

$$\left. + \frac{1}{\mu_2} \left[-G e^{-\mu_2 x} + G + H e^{\mu_2 x} - H \right] + \frac{Dx}{C} \right)$$

$$u_p{}^x = \frac{1}{E_p} \int_0^x \sigma_p{}^x \, dx = \frac{1}{YE_p} \left\{ A(-\mu_1 E e^{-\mu_1 x} + \mu_1 F e^{-\mu_1(L-x)} - \mu_2 G e^{-\mu_2 x} \right.$$

$$+ \mu_2 H e^{\mu_2 x}) + \frac{Px}{\pi E_g t_g (2R_p + t_p + t_g)} - \beta E_j u_j{}^x$$

$$\left. + A(\mu_1 E - \mu_1 F e^{-\mu_1 L} + \mu_2 G - \mu_2 H) \right\}$$

$$u_g{}^x = u_p{}^x + \frac{\tau_p}{K} + \frac{t_g}{G_g} \left(\frac{3\tau_p + \tau_j}{8} \right)$$

$$SLIP \equiv \delta \equiv u_j{}^x - u_p{}^x$$

3.2. THREE-DIMENSIONAL AXISYMMETRIC LINEAR MODEL

The method of solution utilized in this model was analogous to that of the one-dimensional model with the additional inclusion of the radial and circumferential normal stresses. Once again the governing equation becomes a fourth order differential equation whick is solved under appropriate boundary conditions.

In addition to the variables defined in the one-dimensional model, the following ones are included in this model:

σ_j^r = Compressive normal stress in radial direction at the jacket-grout interface

σ_j^θ = Normal stress in the jacket in the hoop direction

σ_p^r = Compressive normal stress in radial direction at the pile-grout interface

σ_g^θ = Normal stress in grout in hoop direction

u_j^r = Displacement in jacket in radial direction

u_p^r =   "   " pile   "   "   "

u_g^r =   "   " grout   "   "   "

ν_j = Poisson's ratio for jacket steel

ν_p =   "   "   " pile   "

ν_g =   "   "   " grout layer

In addition to the assumptions of the one-dimensional model, it is assumed herein that the radial stress varies linearly through the thickness of each component, as shown
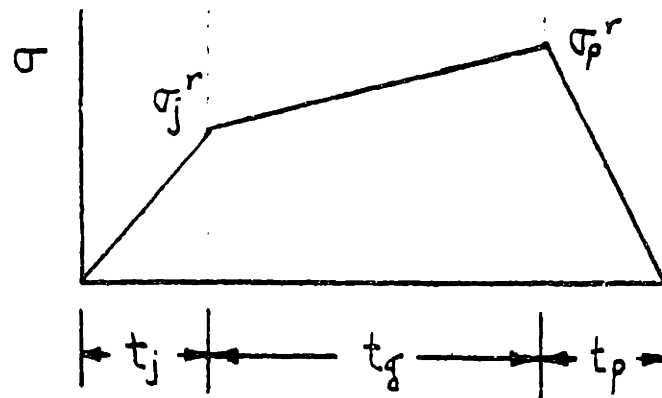
in Figure 3.5.

Figure 3.5. Assumed Distribution of
Compressive Normal Stress in the Radial Direction

Similarly, also assume $u_g^r = \dfrac{u_p^r + u_j^r}{2}$.

Equilibrium

Force equilibrium in the jacket, grout and pile
layers is satisfied in both the vertical and radial
directions. Equilibrium in the hoop direction is satis-
fied automatically by axisymmetry. In the vertical direc-
tion, one obtains the same equilibrium equations as in
the one-dimensional model. In the following, the equili-
brium equations in the radial direction are derived. A
force block diagram accompanies the equation for radial
equilibrium in the jacket.

(1) JACKET

$$\text{VERTICAL:} \quad \left\{ \left(R_j - \frac{t_j}{2} \right) \tau_j = R_j t_j \frac{\partial \sigma_j^x}{\partial x} \right\} \quad (1)$$
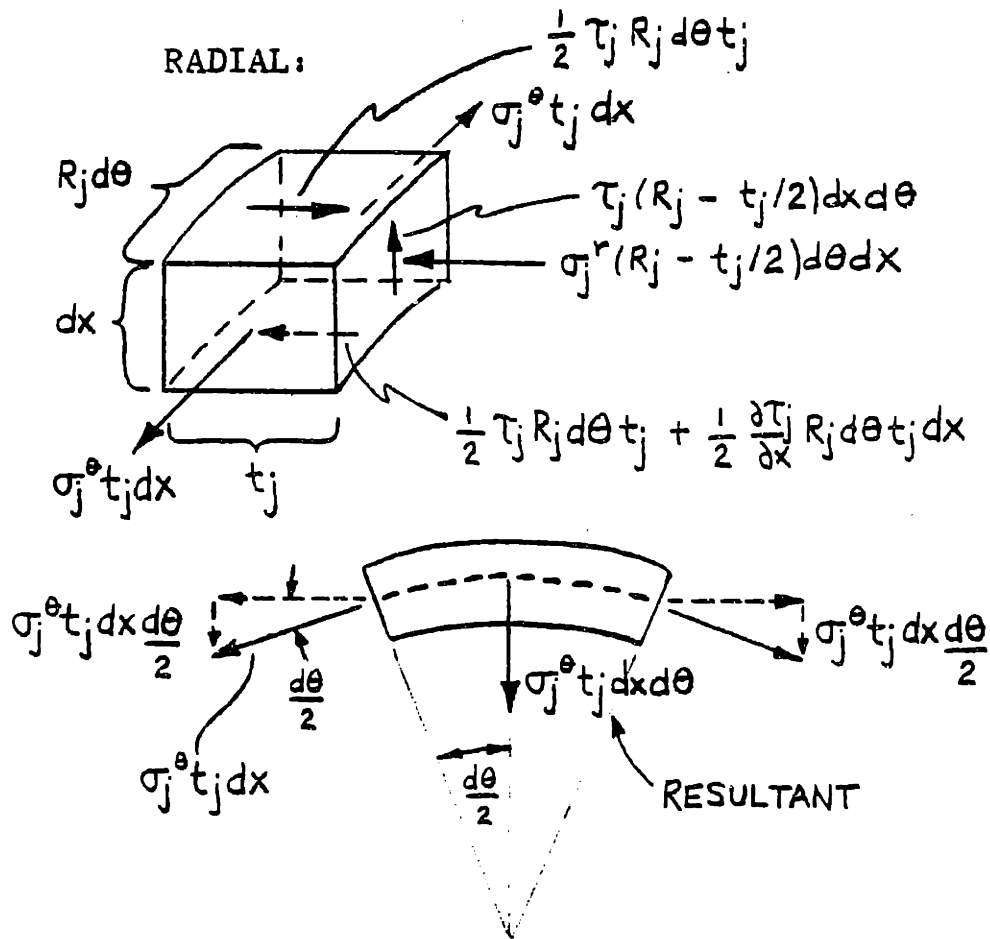
RADIAL:

Therefore, $\left\{ \dfrac{1}{2} \dfrac{\partial \tau_j}{\partial x} R_j t_j + \left(R_j - \dfrac{t_j}{2} \right) \sigma_j^r = \sigma_j^\theta t_j \right\}$ (2)

(2) **GROUT**

VERTICAL:
$$\left\{ \left(R_p + \frac{t_p}{2} \right) \tau_p - \left(R_j - \frac{t_j}{2} \right) \tau_j = \frac{\partial \sigma_g^x}{\partial x} t_g \left(R_p + \frac{t_p + t_g}{2} \right) \right\} \quad (3)$$

RADIAL:
$$\left\{ \frac{1}{2} \left(\frac{\partial \tau_j}{\partial x} + \frac{\partial \tau_p}{\partial x} \right) \left(R_p + \frac{t_p + t_g}{2} \right) t_g - \left(R_j - \frac{t_j}{2} \right) \sigma_j^r + \left(R_p + \frac{t_p}{2} \right) \sigma_p^r = \sigma_g^\theta t_g \right\} \quad (4)$$

(3) **PILE**

VERTICAL: $\left\{ -\left(R_p + \dfrac{t_p}{2} \right) \tau_p = R_p t_p \dfrac{\partial \sigma_p^x}{\partial x} \right\}$ (5)

RADIAL: $\left\{ -\left(R_p + \dfrac{t_p}{2} \right) \sigma_p^r + \dfrac{1}{2} \dfrac{\partial \tau_p}{\partial x} R_p t_p = \sigma_p^\theta t_p \right\}$ (6)

Normal stress-strain relations

(1) <u>JACKET</u>

AXIAL: $\left\{ \dfrac{\partial u_j{}^x}{\partial x} = \dfrac{1}{E_j} \left[\sigma_j{}^x - \nu_j \left(\sigma_j{}^\theta - \sigma_j{}^r/2 \right) \right] \right\}$ (7)

HOOP: $\left\{ \dfrac{u_j{}^r}{R_j} = \dfrac{1}{E_j} \left[\sigma_j{}^\theta - \nu_j \left(\sigma_j{}^x - \sigma_j{}^r/2 \right) \right] \right\}$ (8)

(2) <u>PILE</u>

AXIAL: $\left\{ \dfrac{\partial u_p{}^x}{\partial x} = \dfrac{1}{E_p} \left[\sigma_p{}^x - \nu_p \left(\sigma_p{}^\theta - \sigma_p{}^r/2 \right) \right] \right\}$ (9)

HOOP: $\left\{ \dfrac{u_p{}^r}{R_p} = \dfrac{1}{E_p} \left[\sigma_p{}^\theta - \nu_p \left(\sigma_p{}^x - \sigma_p{}^r/2 \right) \right] \right\}$ (10)

(3) <u>GROUT</u>

AXIAL: $\left\{ \dfrac{\partial \bar{u}_g{}^x}{\partial x} = \dfrac{1}{E_g} \left[\sigma_g{}^x - \nu_g \left(\sigma_g{}^\theta - \left[\dfrac{\sigma_p{}^r + \sigma_j{}^r}{2} \right] \right) \right] \right\}$ (11)

(Notice the use of the average value of $u_g{}^x$, $\bar{u}_g{}^x$, in this equation as was the case in the one-dimensional formulation.)

HOOP: $\left\{ \dfrac{u_g{}^r}{\left(R_p + \dfrac{t_p + t_g}{2} \right)} = \dfrac{1}{E_g} \left[\sigma_g{}^\theta - \nu_g \left(\sigma_g{}^x - \dfrac{\sigma_p{}^r + \sigma_j{}^r}{2} \right) \right] \right\}$ (12)

RADIAL: $\left\{ \dfrac{u_j{}^r - u_p{}^r}{t_g} = \dfrac{1}{E_g} \left[-\left(\dfrac{\sigma_p{}^r + \sigma_j{}^r}{2} \right) - \nu_g \left(\sigma_g{}^x + \sigma_g{}^\theta \right) \right] \right\}$ (13)

Shear stress-strain relations

Again τ varies linearly from τ_j to τ_p, as in the one-dimensional model. Then:

$$\left\{ u_g{}^x - u_{p,g}{}^x = \dfrac{t_g}{G_g} \left(\dfrac{3\tau_p + \tau_j}{8} \right) \right\}$$ (15a)

$$\left\{ \overline{u_g}^x = \frac{u_{j,g}{}^x + 4u_g{}^x + u_{p,g}{}^x}{6} \right\} \quad (15b)$$

$$\left\{ \frac{\tau_j + \tau_p}{2} = \frac{G_g}{t_g}\left(u_{j,g}{}^x - u_{p,g}{}^x \right) \right\} \quad (16)$$

Shear stress-slip relation at interfaces

We take into account the slippage at the interfaces and let the stiffness derived from the bond stress-slip curve be expressed as K. Then --

$$\left\{ u_j{}^x = u_{j,g}{}^x + \tau_j / K \right\} \quad (A)$$

$$\left\{ u_p{}^x = u_{p,g}{}^x - \tau_p / K \right\} \quad (B)$$

Mathematical Solution

Substituting for $u_g{}^r$ into equation (12) one obtains--

$$\frac{u_p{}^r + u_j{}^r}{2R_p + t_p + t_g} = \frac{1}{E_g}\left[\sigma_g{}^\theta - \nu_g \left(\sigma_g{}^x - \left[\frac{\sigma_p{}^r + \sigma_j{}^r}{2} \right] \right) \right]$$

Combining this expression with equation (13), one is able to solve for $u_p{}^r$ and $u_j{}^r$:

$$u_p{}^r = \frac{1}{2E_g}\left\{ (2R_p + t_p + t_g + \nu_g t_g)\sigma_g{}^\theta + (-2R_p\nu_g - t_p\nu_g)\sigma_g{}^x \right.$$
$$\left. + \left[\frac{(2R_p + t_p + t_g)\nu_g + t_g}{2} \right]\sigma_p{}^r + \left[\frac{(2R_p + t_p + t_g)\nu_g + t_g}{2} \right]\sigma_j{}^r \right\}$$

$$u_j{}^r = \frac{1}{2E_g}\left\{ \left[\frac{-t_g}{2} + \frac{\nu_g}{2}(2R_p + t_p + t_g) \right]\sigma_p{}^r + \left[\frac{-t_g}{2} + \frac{\nu_g}{2}(2R_p + t_p + t_g) \right]\sigma_j{}^r \right.$$
$$\left. + \left[-2\nu_g t_g - 2\nu_g R_p - \nu_g t_p \right]\sigma_g{}^x + \left[-\nu_g t_g + 2R_p + t_p + t_g \right]\sigma_g{}^\theta \right\}$$

Combining with equations (8) and (9) we find:

$$\left\{ \frac{R_j}{E_j}\left[\sigma_j{}^\theta - \nu_j\sigma_j{}^x + \frac{\nu_j\sigma_j{}^r}{2}\right] = \frac{1}{2E_q}\left(\left[\frac{-t_q}{2} + \frac{\nu_q}{2}(2R_p + t_p + t_q)\right]\sigma_p{}^r \right.\right.$$

$$\left. + \left[\frac{-t_q}{2} + \frac{\nu_q}{2}(2R_p + t_p + t_q)\right]\sigma_j{}^r + \left[-2\nu_q t_q - 2\nu_q R_p - \nu_q t_p\right]\sigma_q{}^x + \left[\begin{array}{c}-\nu_q t_q + 2R_p \\ + t_p + t_q\end{array}\right]\sigma_q{}^\theta\right)\right\} \quad (17)$$

and

$$\left\{ \frac{R_p}{E_p}\left[\sigma_p{}^\theta - \nu_p\sigma_p{}^x + \frac{\nu_p\sigma_p{}^r}{2}\right] = \frac{1}{2E_q}\left(\left[2R_p + t_p + t_q + \nu_q t_q\right]\sigma_q{}^\theta + \left[-2R_p\nu_q - t_p\nu_q\right]\sigma_q{}^x\right.\right.$$

$$\left. + \left[\frac{(2R_p + t_p + t_q)\nu_q + t_q}{2}\right]\sigma_p{}^r + \left[\frac{(2R_p + t_p + t_q)\nu_q + t_q}{2}\right]\sigma_j{}^r\right)\right\} \quad (18)$$

Combining equation (11) with equations (B), (15b), (15a), (16) and (9) one obtains:

EQN. (19)

$$\left\{ \frac{1}{E_q}\left[\sigma_q{}^x - \nu_q\sigma_q{}^\theta + \frac{\nu_q\sigma_p{}^r}{2} + \frac{\nu_q\sigma_j{}^r}{2}\right] = \left(\frac{1}{E_p}\left[\sigma_p{}^x - \nu_p\sigma_p{}^\theta + \frac{\nu_p\sigma_p{}^r}{2}\right] + \frac{1}{K}\frac{\partial \tau_p}{\partial x} + \frac{t_q}{G_q}\frac{d}{dx}\left(\frac{\tau_j + 2\tau_p}{6}\right)\right)\right\}$$

Substituting for τ_j and τ_p from equations (1) and (5) into equation (16) and then making appropriate substitutions from equations (A), (B), (7) and (9) into equation (16) one finds:

$$\left\{ \frac{G_q}{t_q}\left[\frac{1}{E_j}\left(\sigma_j{}^x - \nu_j\sigma_j{}^\theta + \frac{\nu_j\sigma_j{}^r}{2}\right) - \frac{1}{E_p}\left(\sigma_p{}^x - \nu_p\sigma_p{}^\theta\right.\right.\right.$$

$$\left.\left.\left. + \frac{\nu_p\sigma_p{}^r}{2}\right) - \frac{1}{K}\left(\frac{\partial \tau_j}{\partial x} + \frac{\partial \tau_p}{\partial x}\right)\right] = \frac{1}{2}\left[\left(\frac{2R_j t_j}{2R_j - t_j}\right)\frac{\partial^2\sigma_j{}^x}{\partial x^2} - \left(\frac{2R_p t_p}{2R_p + t_p}\right)\frac{\partial^2\sigma_p{}^x}{\partial x^2}\right]\right\} \quad (20)$$

Adding equations (1), (3) and (5) and integrating, we obtain:

$$\left\{ R_j t_j\sigma_j{}^x + \left[R_p + \frac{t_p + t_q}{2}\right]t_q\sigma_q{}^x + R_p t_p\sigma_p{}^x = \frac{P}{2\pi}\right\} \quad (21)$$

Substituting for $\frac{\partial \tau_j}{\partial x}$ and $\frac{\partial \tau_p}{\partial x}$ from equations (2) and (6) into equation (4):

$$\left\{ \left[t_q\left(\frac{2R_p + t_p + t_q}{2R_j}\right)\right]\sigma_j{}^\theta - \left[\frac{t_q(2R_p + t_p + t_q)(2R_j - t_j)}{4R_j t_j} + \left(R_j - \frac{t_j}{2}\right)\right]\sigma_j{}^r\right.$$

$$\left. + \left[\frac{t_q(2R_p + t_p + t_q)}{2R_p}\right]\sigma_p{}^\theta + \left[\frac{t_q(2R_p + t_p + t_q)(2R_p + t_p)}{4R_p t_p} + \left(R_p + \frac{t_p}{2}\right)\right]\sigma_p{}^r = t_q\sigma_q{}^\theta\right\} \quad (22)$$

Substituting for τ_j from equation (1) into equation (2) one obtains:

$$\left\{ \frac{\partial^2 \sigma_j^x}{\partial x^2} = \left[\frac{2R_j - t_j}{t_j R_j^2}\right]\sigma_j^\theta - \left[\frac{(2R_j - t_j)^2}{2(R_j t_j)^2}\right]\sigma_j^r \right\} \quad (23)$$

Substituting for τ_p from equation (5) into equation (6) yields:

$$\left\{ \frac{\partial^2 \sigma_p^x}{\partial x^2} = -\left(\left[\frac{2R_p + t_p}{t_p R_p^2}\right]\sigma_p^\theta + \left[\frac{(2R_p + t_p)^2}{2(R_p t_p)^2}\right]\sigma_p^r\right) \right\} \quad (24)$$

Substituting from equation (23) and equation (24) into equation (20), one obtains:

$$\left\{ \left(\frac{G_g}{t_g E_j}\right)\sigma_j^x - \left(\frac{G_g}{t_g E_p}\right)\sigma_p^x = \right.$$

$$\left(\frac{G_g \nu_j}{t_g E_j} + \frac{1}{R_j}\left[1 + \frac{2G_g}{kt_g}\right]\right)\sigma_j^\theta - \left(\frac{G_g \nu_j}{2E_j t_g} + \left[\frac{2R_j - t_j}{2R_j t_j}\right]\left[1 + \frac{2G_g}{kt_g}\right]\right)\sigma_j^r + \left(\frac{-G_g \nu_p}{t_g E_p} + \frac{1}{R_p}\left[1 + \frac{2G_g}{kt_g}\right]\right)\sigma_p^\theta$$

$$\left. + \left(\frac{G_g \nu_p}{2E_p t_g} + \left[\frac{2R_p + t_p}{2R_p t_p}\right]\left[1 + \frac{2G_g}{kt_g}\right]\right)\sigma_p^r \right\} \quad (25)$$

Substituting from equation (23) and equation (24) into equation (19), we find:

EQN. (26) ➘

$$\left\{ \frac{\sigma_j^x}{E_g} - \frac{\sigma_p^x}{E_p} = \left(\frac{\nu_g}{E_g}\right)\sigma_j^\theta + \left(\frac{-\nu_g}{2E_g} + \frac{\nu_p}{2E_p}\right.\right.$$

$$\left. + \left[\frac{1}{K} + \frac{t_g}{3G_g}\right]\left[\frac{2R_p + t_p}{R_p t_p}\right]\right)\sigma_p^r + \left(\frac{-\nu_g}{2E_g} - \frac{t_g}{6G_g}\left[\frac{2R_j - t_j}{R_j t_j}\right]\right)\sigma_j^r + \left(\frac{\nu_p}{E_p} + \frac{2}{R_p}\left[\frac{1}{K} + \frac{t_g}{3G_g}\right]\right)\sigma_p^\theta + \frac{t_g}{3G_g R_j}\sigma_j^\theta \right\}$$

Substituting σ_g^x from equation (21) into equations (26), (18) and (17), we eliminate σ_g^x from those equations. The essential equations are therefore the five algebraic equations (26), (25), (22), (18) and (17) and the two differential equations (23) and (24). Using the five algebraic equations, one can solve for the unknowns σ_p^r, σ_p^θ, σ_j^r, σ_j^θ, σ_g^θ in terms of σ_j^x and σ_p^x. Then by substituting those unknowns into equations (23) and (24), one is able to solve the differential equations simultaneously. The five algebraic equations written in matrix form become:

$$\begin{Bmatrix} \sigma_P^r \\ \sigma_P^\theta \\ \sigma_J^r \\ \sigma_J^\theta \\ \sigma_g^\theta \end{Bmatrix} = M\sigma_J^x + N\sigma_P^x + P$$

EQN. NO.					
(25)	$\dfrac{G_g \nu_P}{2E_P t_g} \left(1+\dfrac{2G_g}{kt_g}\right)\dfrac{(2R_P+t_P)(2R_P+t_P)}{(2R_P t_P)} + \dfrac{t_g(2R_P+t_P+t_g)(2R_P+t_P)}{4R_P t_P}$	$\dfrac{-G_g \nu_P}{t_g E_P}\left(1+\dfrac{2G_g}{kt_g}\right)+\dfrac{1}{R_P}$	$-\left(\dfrac{G_g \nu_J}{2E_J t_g}\right)\left[\dfrac{\left(1+\dfrac{2G_g}{kt_g}\right)(2R_J-t_J)}{2R_J t_J}\right]-\left(R_J-\dfrac{t_J}{2}\right)\dfrac{t_g(2R_P+t_P+t_g)(2R_J-t_J)}{4R_J t_J}$	$\dfrac{G_g \nu_J}{t_g E_J}\left(1+\dfrac{2G_g}{kt_g}\right)+\dfrac{1}{R_J}$	0
(22)	$\dfrac{2R_P+t_P}{2} + \dfrac{t_g(2R_P+t_P+t_g)}{2R_P}$	$-\left(\dfrac{1}{K}+\dfrac{t_g}{3G_g}\right)\dfrac{2}{R_P}$	$\dfrac{\nu_g/2E_g}{} + \dfrac{t_g}{6G_g}\left[\dfrac{2R_J-t_J}{R_J t_J}\right]+\dfrac{t_g(2R_P+t_P+t_g)}{2R_J}\left[\dfrac{2R_J-t_J}{R_J t_J}\right]$	$-\dfrac{t_g}{3G_g R_J}$	$-t_g$
(26)	$\dfrac{\nu_g}{2E_g} - \dfrac{\nu_P}{2E_P}$	$-\nu_P/E_P$	$-\left(\dfrac{1}{K}+\dfrac{t_g}{3G_g}\right)\dfrac{2}{R_P}$		$-\dfrac{\nu_g}{E_g}$
(18)	$\dfrac{\nu_P R_P}{2E_P}$	$\dfrac{R_P}{E_P}$	$\dfrac{R_J \nu_J}{2E_J} + \dfrac{t_g}{4E_g} - \dfrac{\nu_g(2R_P+t_P+t_g)\nu_g}{4E_g}$	0	$\dfrac{\nu_g t_g}{2E_g} - \dfrac{R_P}{E_g}$
(17)	$-\dfrac{[2R_P+t_P+t_g]\nu_g+t_g}{4E_g} - \dfrac{1}{2E_g}\left(-\dfrac{t_g}{2}\right)+\dfrac{\nu_g[2R_P+t_P+t_g]}{2}$	0	$-\left[\dfrac{2R_P+t_P+t_g}{4E_g}\right]+\dfrac{t_g}{4E_g}$	$\dfrac{R_J}{E_J}$	$-\left[\dfrac{2R_P+t_P+t_g+\nu_g t_g}{2E_g}\right] - \dfrac{t_P}{2E_g}$

$A2$

$$\text{where} \quad \underset{\sim}{M} = \begin{bmatrix} \dfrac{G_q}{t_q E_j} \\[2mm] 0 \\[2mm] \dfrac{2R_j t_j}{t_q E_q (2R_p + t_p + t_q)} \\[3mm] \left(\dfrac{2R_p \nu_q + t_p \nu_q}{2E_q}\right)\left(\dfrac{2R_j t_j}{t_q [2R_p + t_p + t_q]}\right) \\[3mm] \left(\dfrac{\nu_q t_q}{E_q} + \dfrac{\nu_q R_p}{E_q} + \dfrac{\nu_q t_p}{2E_q}\right)\left(\dfrac{2R_j t_j}{t_q (2R_p + t_p + t_q)}\right) + \dfrac{R_j \nu_j}{E_j} \end{bmatrix}$$

$$\underset{\sim}{N} = \begin{bmatrix} \dfrac{-G_q}{t_q E_p} \\[2mm] 0 \\[2mm] \dfrac{1}{E_p} + \dfrac{2R_p t_p}{t_q E_q (2R_p + t_p + t_q)} \\[3mm] \dfrac{\nu_p R_p}{E_p} + \left(\dfrac{2R_p \nu_q + t_p \nu_q}{2E_q}\right)\left(\dfrac{2R_p t_p}{t_q (2R_p + t_p + t_q)}\right) \\[3mm] \left(\dfrac{\nu_q t_q}{E_q} + \dfrac{\nu_q R_p}{E_q} + \dfrac{\nu_q t_p}{2E_q}\right)\left(\dfrac{2R_p t_p}{t_q [2R_p + t_p + t_q]}\right) \end{bmatrix}$$

$$\underset{\sim}{P} = \begin{bmatrix} 0 \\[2mm] 0 \\[2mm] \dfrac{-P}{\pi E_q (2R_p + t_p + t_q) t_q} \\[3mm] -\left(\dfrac{2R_p \nu_q + t_p \nu_q}{2E_q}\right)\left(\dfrac{P}{\pi t_q (2R_p + t_p + t_q)}\right) \\[3mm] -\left(\dfrac{\nu_q t_q}{E_q} + \dfrac{\nu_q R_p}{E_q} + \dfrac{\nu_q t_p}{2E_q}\right)\left(\dfrac{P}{\pi t_q (2R_p + t_p + t_q)}\right) \end{bmatrix}$$

$$\text{Let} \quad \begin{Bmatrix} a_1 \\ a_2 \\ a_3 \\ a_4 \\ a_5 \end{Bmatrix} = \underset{\sim}{A}^{-1}\underset{\sim}{M}, \quad \begin{Bmatrix} b_1 \\ b_2 \\ b_3 \\ b_4 \\ b_5 \end{Bmatrix} = \underset{\sim}{A}^{-1}\underset{\sim}{N}, \quad \begin{Bmatrix} c_1 \\ c_2 \\ c_3 \\ c_4 \\ c_5 \end{Bmatrix} = \underset{\sim}{A}^{-1}\underset{\sim}{P}$$

$$\therefore \quad \sigma_p^{\,r} = a_1 \sigma_j^{\,x} + b_1 \sigma_p^{\,x} + c_1$$
$$\sigma_p^{\,\theta} = a_2 \sigma_j^{\,x} + b_2 \sigma_p^{\,x} + c_2$$
$$\sigma_j^{\,r} = a_3 \sigma_j^{\,x} + b_3 \sigma_p^{\,x} + c_3$$
$$\sigma_j^{\,\theta} = a_4 \sigma_j^{\,x} + b_4 \sigma_p^{\,x} + c_4$$
$$\sigma_q^{\,\theta} = a_5 \sigma_j^{\,x} + b_5 \sigma_p^{\,x} + c_5$$

Substituting these into equations (23) and (24):

Equation (23)*

$$\frac{\partial^2 \sigma_j^x}{\partial x^2} = \left\{ \left[\frac{2R_j - t_j}{t_j R_j^2} \right] a_4 - \frac{(2R_j - t_j)^2 a_3}{2(R_j t_j)^2} \right\} \sigma_j^x$$

$$+ \left\{ \left(\frac{2R_j - t_j}{t_j R_j^2} \right) b_4 - \frac{(2R_j - t_j)^2 b_3}{2(R_j t_j)^2} \right\} \sigma_p^x + \left\{ \frac{(2R_j - t_j) c_4}{t_j R_j^2} - \frac{(2R_j - t_j)^2 c_3}{2(R_j t_j)^2} \right\}$$

$$\therefore \frac{\partial^4 \sigma_j^x}{\partial x^4} = \left\{ \left(\frac{2R_j - t_j}{t_j R_j^2} \right) a_4 - \frac{(2R_j - t_j)^2 a_3}{2(R_j t_j)^2} \right\} \frac{\partial^2 \sigma_j^x}{\partial x^2} + \left\{ \left(\frac{2R_j - t_j}{t_j R_j^2} \right) b_4 - \frac{(2R_j - t_j)^2 b_3}{2(R_j t_j)^2} \right\} \frac{\partial^2 \sigma_p^x}{\partial x^2}$$

Equation (24)*

$$\frac{\partial^2 \sigma_p^x}{\partial x^2} = \left\{ \frac{-(2R_p + t_p) a_2}{t_p R_p^2} - \frac{(2R_p + t_p)^2 a_1}{2(R_p t_p)^2} \right\} \sigma_j^x + \left\{ \frac{-(2R_p + t_p) b_2}{t_p R_p^2} - \frac{(2R_p + t_p)^2 b_1}{2(R_p t_p)^2} \right\} \sigma_p^x$$

$$+ \left\{ \frac{-(2R_p + t_p) c_2}{t_p R_p^2} - \frac{(2R_p + t_p)^2 c_1}{2(R_p t_p)^2} \right\}$$

Substituting $\frac{\partial^2 \sigma_p^x}{\partial x^2}$ into the equation for $\frac{\partial^4 \sigma_j^x}{\partial x^4}$ one finds:

$$\frac{\partial^4 \sigma_j^x}{\partial x^4} = \left\{ \left(\frac{2R_j - t_j}{t_j R_j^2} \right) a_4 - \frac{(2R_j - t_j)^2 a_3}{2(R_j t_j)^2} \right\} \frac{\partial^2 \sigma_j^x}{\partial x^2} + \left\{ \left(\frac{2R_j - t_j}{\tau_j R_j^2} \right) b_4 - \frac{(2R_j - t_j)^2 b_3}{2(R_j t_j)^2} \right\} \left\{ \frac{-(2R_p + t_p) c_2}{t_p R_p^2} - \frac{(2R_p + t_p)^2 c_1}{2(R_p t_p)^2} \right\}$$

$$+ \left\{ \left(\frac{2R_j - t_j}{t_j R_j^2} \right) b_4 - \frac{(2R_j - t_j)^2 b_3}{2(R_j t_j)^2} \right\} \left\{ \frac{-(2R_p + t_p) a_2}{t_p R_p^2} - \frac{(2R_p + t_p)^2 a_1}{2(R_p t_p)^2} \right\} \sigma_j^x$$

$$+ \left\{ \left(\frac{2R_j - t_j}{t_j R_j^2} \right) b_4 - \frac{(2R_j - t_j)^2 b_3}{2(R_j t_j)^2} \right\} \left\{ \frac{-(2R_p + t_p) b_2}{t_p R_p^2} - \frac{(2R_p + t_p)^2 b_1}{2(R_p t_p)^2} \right\} \sigma_p^x$$

Now substituting σ_p^x from equation (23)* into the above; one obtains:

$$\frac{\partial^4 \sigma_j^x}{\partial x^4} = \left[\left(\frac{-(2R_p + t_p) b_2}{t_p R_p^2} - \frac{(2R_p + t_p)^2 b_1}{2(R_p t_p)^2} + \frac{(2R_j - t_j) a_4}{t_j R_j^2} - \frac{(2R_j - t_j)^2 a_3}{2(R_j t_j)^2} \right) \right] \frac{\partial^2 \sigma_j^x}{\partial x^2}$$

$$+ \left[\left(\frac{(2R_p + t_p) b_2}{t_p R_p^2} + \frac{(2R_p + t_p)^2 b_1}{2(R_p t_p)^2} \right) \left\{ \frac{(2R_j - t_j) c_4}{t_j R_j^2} - \frac{(2R_j - t_j)^2 c_3}{2(R_j t_j)^2} \right\} \right.$$

$$\left. + \left\{ \frac{(2R_j - t_j) b_4}{t_j R_j^2} - \frac{(2R_j - t_j)^2 b_3}{2(R_j t_j)^2} \right\} \left\{ \frac{-(2R_p + t_p) c_2}{t_j R_p^2} - \frac{(2R_p + t_p)^2 c_1}{2(R_p t_p)^2} \right\} \right] \quad \text{(CONT'D)}$$

$$+ \left[\left\{\frac{(2R_j - t_j)b_4}{t_j R_j^2} - \frac{(2R_j - t_j)^2 b_3}{2(R_j t_j)^2}\right\}\left\{\frac{-(2R_p + t_p)a_2}{t_p R_p^2} - \frac{(2R_p + t_p)^2 a_1}{2(R_p t_p)^2}\right\}\right.$$

$$\left.+ \left\{\frac{(2R_p + t_p)b_2}{t_p R_p^2} + \frac{(2R_p + t_p)^2 b_1}{2(R_p t_p)^2}\right\}\left\{\frac{(2R_j - t_j)a_4}{t_j R_j^2} - \frac{(2R_j - t_j)^2 a_3}{2(R_j t_j)^2}\right\}\right]\sigma_j^x$$

Let $B \equiv \left\{\dfrac{-(2R_p + t_p)b_2}{t_p R_p^2} - \dfrac{(2R_p + t_p)^2 b_1}{2(R_p t_p)^2} + \dfrac{(2R_j - t_j)a_4}{t_j R_j^2} - \dfrac{(2R_j - t_j)^2 a_3}{2(R_j t_j)^2}\right\}$

$C \equiv \left\{\dfrac{(2R_j - t_j)b_4}{t_j R_j^2} - \dfrac{(2R_j - t_j)^2 b_3}{2(R_j t_j)^2}\right\}\left\{\dfrac{-(2R_p + t_p)a_2}{t_p R_p^2} - \dfrac{(2R_p + t_p)^2 a_1}{2(R_p t_p)^2}\right\}$

$\qquad + \left\{\dfrac{(2R_p + t_p)b_2}{t_p R_p^2} + \dfrac{(2R_p + t_p)^2 b_1}{2(R_p t_p)^2}\right\}\left\{\dfrac{(2R_j - t_j)a_4}{t_j R_j^2} - \dfrac{(2R_j - t_j)^2 a_3}{2(R_j t_j)^2}\right\}$

$D \equiv \left\{\dfrac{(2R_p + t_p)b_2}{t_p R_p^2} + \dfrac{(2R_p + t_p)^2 b_1}{2(R_p t_p)^2}\right\}\left\{\dfrac{(2R_j - t_j)c_4}{t_j R_j^2} - \dfrac{(2R_j - t_j)^2 c_3}{2(R_j t_j)^2}\right\}$

$\qquad + \left\{\dfrac{(2R_j - t_j)b_4}{t_j R_j^2} + \dfrac{(2R_j - t_j)^2 b_3}{2(R_j t_j)^2}\right\}\left\{\dfrac{-(2R_p + t_p)c_2}{t_p R_p^2} - \dfrac{(2R_p + t_p)^2 c_1}{2(R_p t_p)^2}\right\}$

Therefore $\dfrac{\partial^4 \sigma_j^x}{\partial x^4} - B\dfrac{\partial^2 \sigma_j^x}{\partial x^2} - C\sigma_j^x = D$ becomes the governing equation and the solution is of the form:

$$\sigma_j^x = Ee^{-\mu_1 x} + Fe^{\mu_1 x} + Ge^{-\mu_2 x} + He^{\mu_2 x} - D/C$$

where $\mu_1^2 = \dfrac{B + \sqrt{B^2 + 4C}}{2}$ and $\mu_2^2 = \dfrac{B - \sqrt{B^2 + 4C}}{2}$

$$\therefore \mu_1 = \sqrt{\frac{B + \sqrt{B^2 + 4C}}{2}} \qquad \mu_2 = \sqrt{\frac{B - \sqrt{B^2 + 4C}}{2}}$$

Using boundary conditions to solve for the coefficients --

At $x = 0$, $\sigma_j^x = \dfrac{P}{2\pi R_j t_j} = E + F + G + H - \dfrac{D}{C}$

At $x = L$, $\sigma_j^x = 0 = Ee^{-\mu_1 L} + Fe^{\mu_1 L} + Ge^{-\mu_2 L} + He^{\mu_2 L} - \dfrac{D}{C}$.

At $x = 0$, $\sigma_p^x = 0$

$\therefore \mu_1^2 E + \mu_1^2 F + \mu_2^2 G + \mu_2^2 H = \left\{ \dfrac{(2R_j' - t_j)C_4}{t_j R_j'^2} - \dfrac{(2R_j' - t_j)^2 C_3}{2(R_j' t_j)^2} \right\}$

$\qquad\qquad\qquad\qquad\qquad + \left\{ \left(\dfrac{2R_j' - t_j}{t_j R_j'^2}\right) a_4 - \dfrac{(2R_j' - t_j)^2 a_3}{2(R_j' t_j)^2} \right\} \left\{ E + F \right.$

$\qquad\qquad\qquad\qquad\qquad\qquad \left. + G + H - D/C \right\}$

At $x = L$, $\sigma_p^x = \dfrac{P}{2\pi R_p t_p}$

$\therefore \mu_1^2 E e^{-\mu_1 L} + \mu_1^2 F e^{\mu_1 L} + \mu_2^2 G e^{-\mu_2 L} + \mu_2^2 H e^{\mu_2 L}$

$= \left\{ \left(\dfrac{2R_j - t_j}{t_j R_j^2}\right) a_4 - \dfrac{(2R_j - t_j)^2 a_3}{2(R_j t_j)^2} \right\} \left\{ E e^{-\mu_1 L} + F e^{\mu_1 L} + G e^{-\mu_2 L} + H e^{\mu_2 L} - D/C \right\}$

$+ \left\{ \left(\dfrac{2R_j - t_j}{t_j R_j^2}\right) b_4 - \dfrac{(2R_j - t_j)^2 b_3}{2(R_j t_j)^2} \right\} \left\{ \dfrac{P}{2\pi R_p t_p} \right\} + \dfrac{(2R_j - t_j)C_4}{t_j R_j^2} - \dfrac{(2R_j - t_j)^2 C_3}{2(R_j t_j)^2}$

In matrix form the equations for the boundary conditions are:

$$
\begin{bmatrix}
1 & 1 & 1 & 1 \\
e^{-\mu_1 L} & e^{\mu_1 L} & e^{-\mu_2 L} & e^{\mu_2 L} \\
\mu_1^2 - W & \mu_1^2 - W & \mu_2^2 - W & \mu_2^2 - W \\
e^{-\mu_1 L}(\mu_1^2 - W) & e^{\mu_1 L}(\mu_1^2 - W) & e^{\mu_2 L}(\mu_2^2 - W) & e^{\mu_2 L}(\mu_2^2 - W)
\end{bmatrix}
\begin{Bmatrix}
E \\ F \\ G \\ H
\end{Bmatrix}
=
\begin{bmatrix}
\dfrac{P}{2\pi R_j t_j} + \dfrac{D}{C} \\[2mm]
\dfrac{D}{C} \\[2mm]
\dfrac{(2R_j - t_j)C_4}{t_j R_j^2} - \dfrac{(2R_j - t_j)^2 C_3}{2(R_j t_j)^2} - \dfrac{DW}{C} \\[2mm]
\dfrac{-DW}{C} + S
\end{bmatrix}
$$

where $W = \left(\dfrac{2R_j - t_j}{t_j R_j^2}\right)a_4 - \dfrac{(2R_j - t_j)^2 a_3}{2(R_j t_j)^2}$

$S = \left\{\left(\dfrac{2R_j - t_j}{t_j R_j^2}\right)b_4 - \dfrac{(2R_j - t_j)^2 b_3}{2(R_j t_j)^2}\right\}\left\{\dfrac{P}{2\pi R_p t_p}\right\}$

$\qquad + \dfrac{(2R_j - t_j)c_4}{t_j R_j^2} - \dfrac{(2R_j - t_j)^2 c_3}{2(R_j t_j)^2}$

Therefore the constants E, F, G and H can be solved by matrix multiplication. The final solution is:

$$\sigma_j^x = Ee^{-\mu_1 x} + Fe^{\mu_1 x} + Ge^{-\mu_2 x} + He^{\mu_2 x} - D/C$$

$$\sigma_p^x = \left[\begin{array}{l} \mu_1^2 Ee^{-\mu_1 x} + \mu_1^2 Fe^{\mu_1 x} + \mu_2^2 Ge^{-\mu_2 x} + \mu_2^2 He^{\mu_2 x} \\[2mm] - \left\{\left(\dfrac{2R_j - t_j}{t_j R_j^2}\right)a_4 - \dfrac{(2R_j - t_j)^2 a_3}{2(R_j t_j)^2}\right\}\sigma_j^x - \dfrac{(2R_j - t_j)c_4}{t_j R_j^2} + \dfrac{(2R_j - t_j)^2 c_3}{2(R_j t_j)^2} \end{array}\right]$$
$$\Bigg/ \left[\left(\dfrac{2R_j - t_j}{t_j R_j^2}\right)b_4 - \dfrac{(2R_j - t_j)^2 b_3}{2(R_j t_j)^2}\right]$$

$$\sigma_g^x = \dfrac{P}{\pi t_g(2R_p + t_p + t_g)} - \dfrac{2R_j t_j \sigma_j^x}{t_g(2R_p + t_p + t_g)} - \dfrac{2R_p t_p \sigma_p^x}{t_g(2R_p + t_p + t_g)}$$

$$\sigma_j^r = a_3 \sigma_j^x + b_3 \sigma_p^x + c_3$$

$$\sigma_p^r = a_1 \sigma_j^x + b_1 \sigma_p^x + c_1$$

$$\sigma_g^r = (\sigma_j^r + \sigma_p^r)/2$$

$$\sigma_j^\theta = a_4 \sigma_j^x + b_4 \sigma_p^x + c_4$$

$$\sigma_p^\theta = a_2 \sigma_j^x + b_2 \sigma_p^x + c_2$$

$$\sigma_g^\theta = a_5 \sigma_j^x + b_5 \sigma_p^x + c_5$$

$$\tau_j = \frac{R_j t_j}{(R_j - t_j/2)}\left(-\mu_1 E e^{-\mu_1 x} + \mu_1 F e^{\mu_1 x} - \mu_2 G e^{-\mu_2 x} + \mu_2 H e^{\mu_2 x}\right)$$

$$\tau_p = \frac{-R_p t_p}{\left(R_p + \frac{t_p}{2}\right)\left(\left[\frac{2R_j - t_j}{t_j R_j^2}\right]b_4 - \frac{(2R_j - t_j)^2 b_3}{2(R_j t_j)^2}\right)}\left[-\mu_1^3 E e^{-\mu_1 x} + \mu_1^3 F e^{\mu_1 x}\right.$$

$$\left. - \mu_2^3 G e^{-\mu_2 x} + \mu_2^3 H e^{\mu_2 x} - \left\{\left(\frac{2R_j - t_j}{t_j R_j^2}\right)a_4 - \frac{(2R_j - t_j)^2 a_3}{2(R_j t_j)^2}\right\}\left\{\begin{array}{l} -\mu_1 E e^{-\mu_1 x} \\ +\mu_1 F e^{\mu_1 x} \\ -\mu_2 G e^{-\mu_2 x} \\ +\mu_2 H e^{\mu_2 x} \end{array}\right\}\right]$$

$$\tau_g = (\tau_j + \tau_p)/2$$

$$u_j^x = \int_0^x \frac{1}{E_j}\left[\sigma_j^x - \nu_j\left(\sigma_j^\theta - \frac{\sigma_j^r}{2}\right)\right]dx$$

$$= \frac{1}{E_j}\left[\frac{1}{\mu_1}\left(-E e^{-\mu_1 x} + F e^{\mu_1 x} + E - F\right) + \frac{1}{\mu_2}\left(-G e^{-\mu_2 x} + H e^{\mu_2 x} + G - H\right)\right.$$

$$\frac{-Dx}{C} + \nu_j\left(-a_4 + a_3/2\right)\left(\frac{1}{\mu_1}\left\{-E e^{-\mu_1 x} + F e^{\mu_1 x} + E - F\right\}\right.$$

$$\left. + \frac{1}{\mu_2}\left\{-G e^{-\mu_2 x} + H e^{\mu_2 x} + G - H\right\} - \frac{Dx}{C}\right)$$

$$+ \nu_j\left(-b_4 + b_3/2\right)\left(\frac{1}{\left\{\frac{2R_j - t_j}{t_j R_j^2}\right\}b_4 - \frac{(2R_j - t_j)^2}{2(R_j t_j)^2}a_3}\right)\left(-\mu_1 E e^{-\mu_1 x}\right.$$

$$\left. + \mu_1 F e^{\mu_1 x} - \mu_2 G e^{-\mu_2 x} + \mu_2 H e^{\mu_2 x} + \mu_1 E - \mu_1 F + \mu_2 G - \mu_2 H\right.$$

$$-W\left\{\frac{-Ee^{-\mu_1 x}}{\mu_1} + \frac{E}{\mu_1} + \frac{F}{\mu_1}(e^{\mu_1 x}-1) - \frac{G}{\mu_2}(e^{-\mu_2 x}-1) + \frac{H}{\mu_2}(e^{\mu_2 x}-1)\right.$$

$$\left.-\frac{Dx}{C}\right\} - \frac{(2R_j-t_j)C_4 x}{t_j R_j^2} + \frac{(2R_j-t_j)^2 C_3 x}{2(R_j t_j)^2}\right) - V_j C_4 x + \frac{V_j C_3 x}{2}\right]$$

$$u_j^r = \frac{R_j}{E_j}\left(\sigma_j^\theta - V_j\left[\sigma_j^x - \frac{\sigma_j^r}{2}\right]\right)$$

$$u_p^x = \frac{1}{E_p}\int_o^x\left[\sigma_p^x - V_p\left(\sigma_p^\theta - \frac{\sigma_p^r}{2}\right)\right]dx$$

$$= \frac{1}{E_p}\left(\frac{1-V_p b_2 + V_p b_1/2}{\left[\frac{2R_j-t_j}{t_j R_j^2}\right]b_4 - \frac{(2R_j-t_j)^2 b_3}{2(R_j t_j)^2}}\right)\left[-\mu_1 E(e^{-\mu_1 x}-1) + \mu_1 F(e^{\mu_1 x}-1)\right.$$

$$\left.-\mu_2 G(e^{-\mu_2 x}-1) + \mu_2 H(e^{\mu_2 x}-1) - \frac{(2R_j-t_j)C_4 x}{t_j R_j^2} + \frac{(2R_j-t_j)^2 C_3 x}{2(R_j t_j)^2}\right]$$

$$-\frac{1}{E_p}\left\{\left(\frac{W[1-V_p b_2 + V_p b_1/2]}{\left[\frac{2R_j-t_j}{t_j R_j^2}\right]b_4 - \frac{(2R_j-t_j)^2 b_3}{2(R_j t_j)^2}}\right) + \frac{V_p a_1}{2} - V_p a_2\right\}\left\{\frac{-E}{\mu_1}(e^{-\mu_1 x}-1)\right.$$

$$\left.+ \frac{F}{\mu_1}(e^{\mu_1 x}-1) - \frac{G}{\mu_2}(e^{-\mu_2 x}-1) + \frac{H}{\mu_2}(e^{\mu_2 x}-1) - \frac{Dx}{C}\right\}$$

$$-\frac{V_p C_2 x}{E_p} + \frac{V_p C_1 x}{2E_p}$$

$$u_p^r = \frac{R_p}{E_p}\left[\sigma_p^\theta - V_p(\sigma_p^x - \sigma_p^r/2)\right]$$

$$u_g{}^x = u_p{}^x + \frac{\tau_p}{K} + \frac{t_g}{G_g}\left(\frac{3\tau_p + \tau_j}{8}\right)$$

$$u_g{}^r = (u_p{}^r + u_j{}^r)/2$$

Since the model is axisymmetric, $u_j{}^\theta = u_p{}^\theta = u_g{}^\theta = 0$.
The slip is $u_j{}^x - u_p{}^x$.

CHAPTER 4: NUMERICAL MODEL

4.1. FINITE ELEMENT ANALYSIS

A finite element static analysis was performed using
an Automatic Dynamic Incremental Non-linear Analysis pro-
gram (ADINA) developed at M.I.T. In the non-linear static
analysis the finite element system response was evaluated
using an incremental solution of the equations of equili-
brium. The incremental solution scheme used was an acce-
lerated modified Newton iteration. To increase the solu-
tion efficiency and to assure an accurate solution, solu-
tion steps were specified in which a new effective stiff-
ness matrix was formed and equilibrium iterations were
carried out. During the step-by-step solution, the linear
effective stiffness matrix was only updated for the non-
linearities in the system.

The complete solution process consisted of four dis-
tinct phases: the finite element mesh and element data
were prepared and compiled; the constant structure matrices
(in this case the linear structure stiffness matrix only)
were assembled; the externally applied load vectors were
calculated; and then the step-by-step solution was obtained
which provided the displacement vectors as well as element
stresses.

4.2. THE FINITE ELEMENT MODEL

Figure 4 shows the finite element discretization employed in the analysis. This mesh contained 61 isoparametric two-dimensional finite elements to model the jacket steel, pile steel and grout material layers and 160 three-dimensional truss elements to model the two steel-grout interfaces. The model contained 359 node points.

A linear-elastic stress-strain relationship for the two-dimensional elements was used. The displacements of the elements were assumed to be small and the strains infinitesimal. The material behavior of the isotropic model was defined by the constant Young's moduli and Poisson ratios. These values were the same as those used for the analytical models.

A materially non-linear stress-strain relationship was used for the truss elements and followed the assumed non-linear behavior of the bond stress versus slippage curve (Chapter 2) to model the steel-grout interfaces. An elastic-plastic model was used for these truss elements defined in terms of the initial Young's modulus, the yield stress and the strain hardening modulus.

This model was fixed at the top of the jacket steel and incremental prescribed displacements were applied at the bottom of the pile steel.
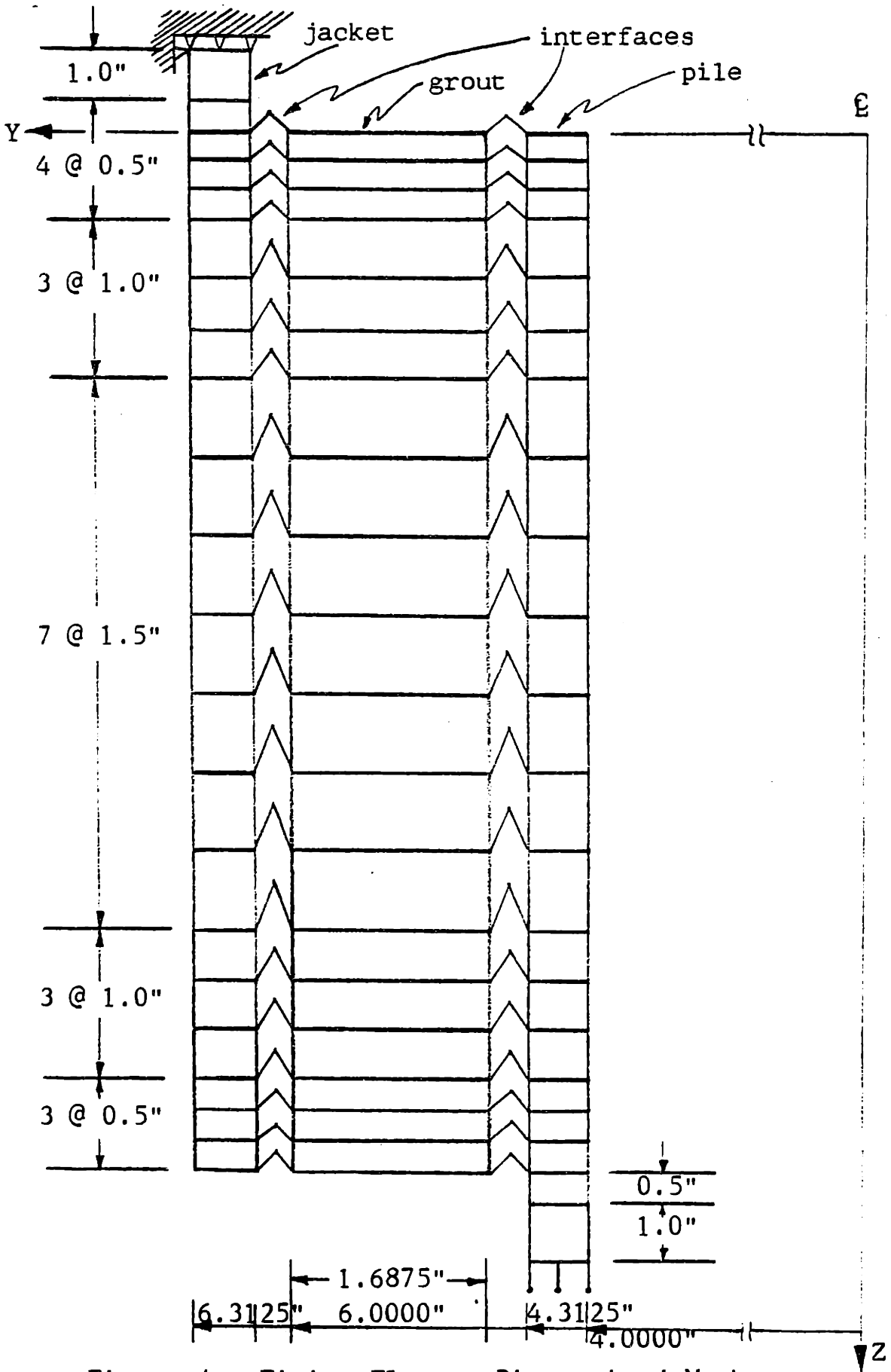
Figure 4. Finite Element Discretized Mesh

CHAPTER 5: RESULTS AND DISCUSSION

The results of the three models employed are pre-
sented in graphical form, accompanied by an analysis and
interpretation. Figure 5.1. shows the plot of bond
strength versus deformation or slip as calculated by
each of the three models as well as the existing experi-
mental data. The bond strength values were obtained by
dividing the applied load on the connection by the total
surface area of the interface, namely the contact area
between the grout and pile surface.

In all three models, the same properties of grout,
radial geometry and stiffness of steel to grout interface
were used. However, Figure 5.1. shows an increase of
overall connection stiffness as the models become more
sophisticated. This effect may be due to the different
distributions of shear stresses along the connection given
by the different models.

Due to the capability of the finite element model to
account for the non-linear behavior of the bond stress
versus deformation relationship, that model provides re-
sults in the plastic range of Figure 5.1. as well.

Figures 5.2, 5.3 and 5.4 give the plots of longitu-
dinal normal stresses σ_j^x, σ_p^x and σ_g^x, respectively, as
a function of position in the material layers. These
graphs describe the distribution of load along the con-
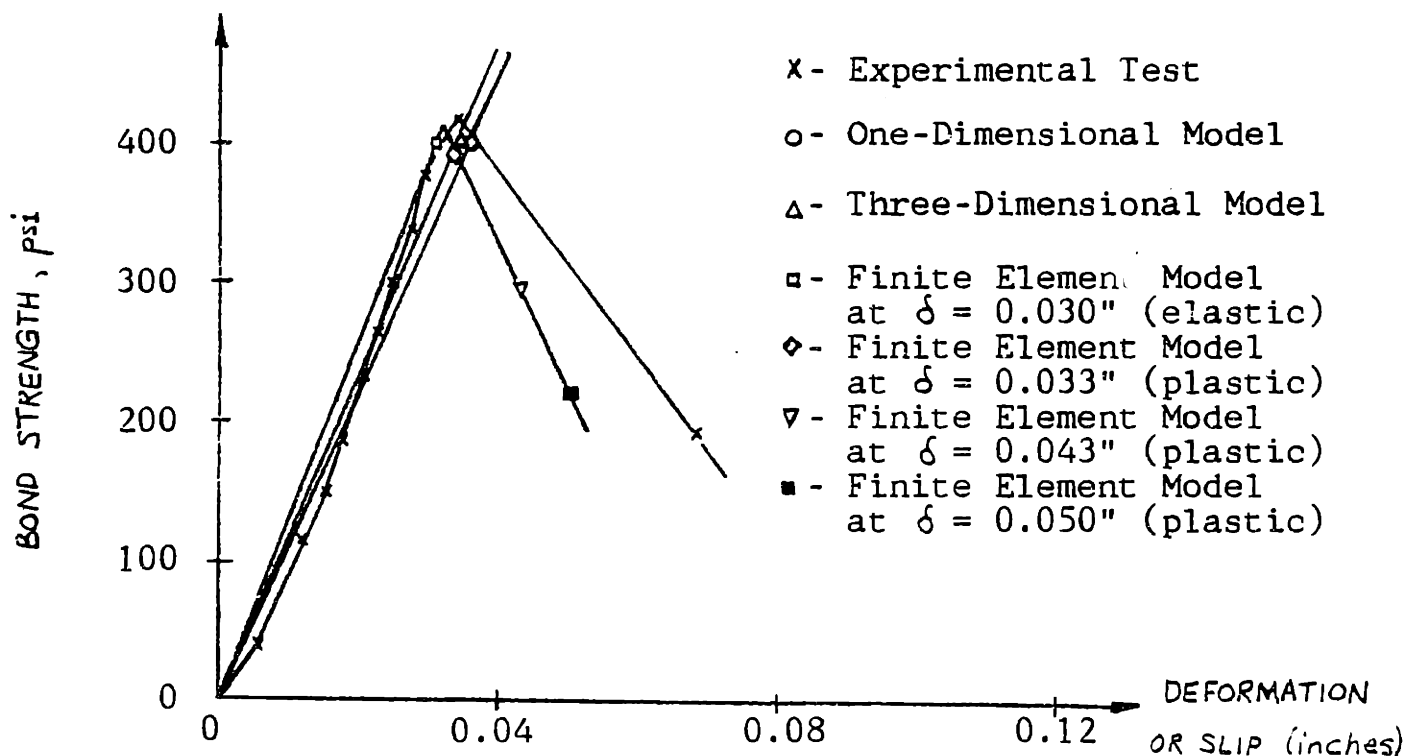
Figure 5.1.   Comparison of Results from Models
and Test of Bond Strength vs. Deformation
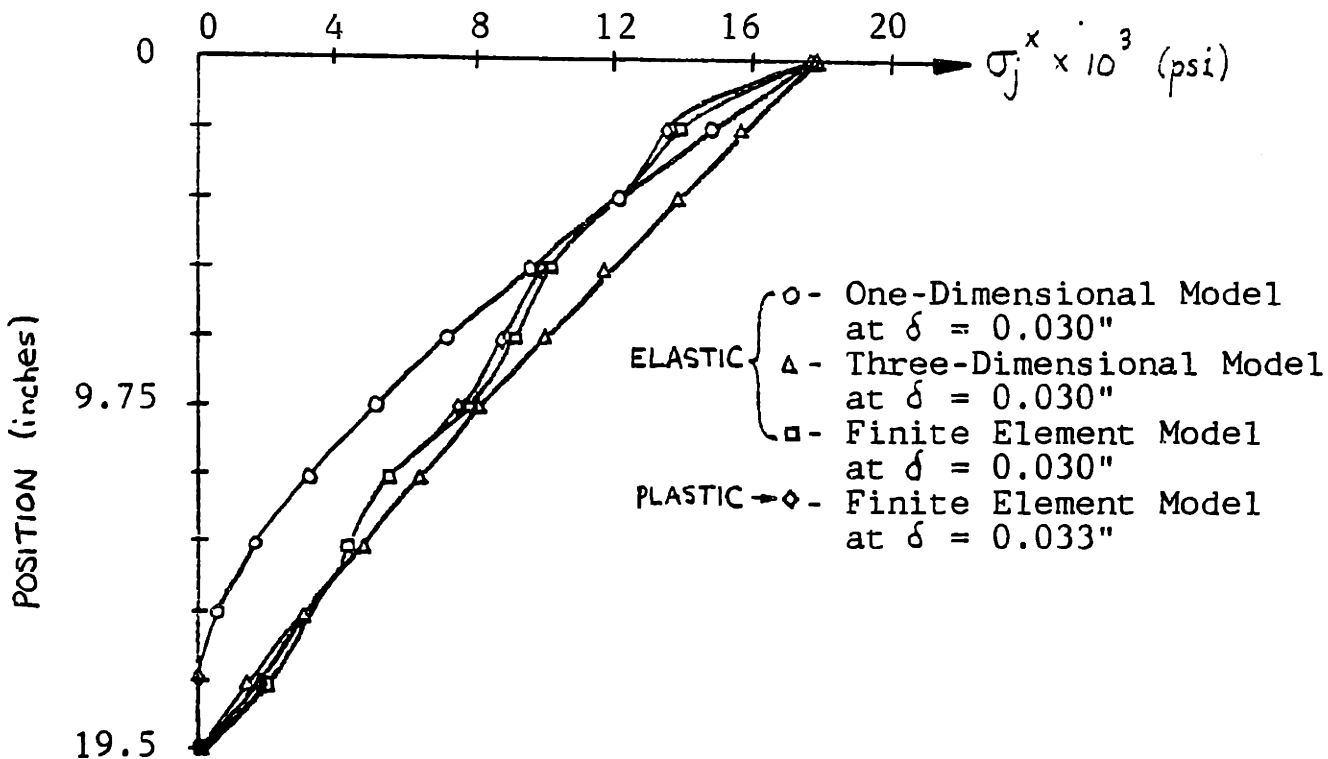
Figure 5.2.   Longitudinal Normal Stress σ_j^x
in the Jacket

nection. As expected, when the load is applied at the top of the jacket steel it is carried completely by the jacket with no stresses seen in the grout or in the pile. The stress in the jacket decreases with distance from the top in an almost linear form whereas the stress in the pile increases in almost linear form as well and the stress in the grout follows a parabolic distribution which reaches a maximum in the middle of the connection and becomes zero at both ends.

The inclusion of Poisson effects in the three-dimensional and the finite element models causes the decay of stress in the jacket steel with distance from the top to lessen and therefore larger stresses are seen in the lower end of the jacket according to those models than those predicted by the one-dimensional model. However the results of all three models for stress in the pile steel are in good agreement. The deviation of the finite element results for stress in the jacket from a smooth , almost linear distribution can be attributed to bending effects in the jacket steel.

The longitudinal normal stress values in the grout as predicted by the three-dimensional and finite element models are in good agreement, however due to the deviation of σ_j^x given by the one-dimensional model from those given by the other two models, the plot of σ_g^x as predicted by the one-dimensional model differs drastically
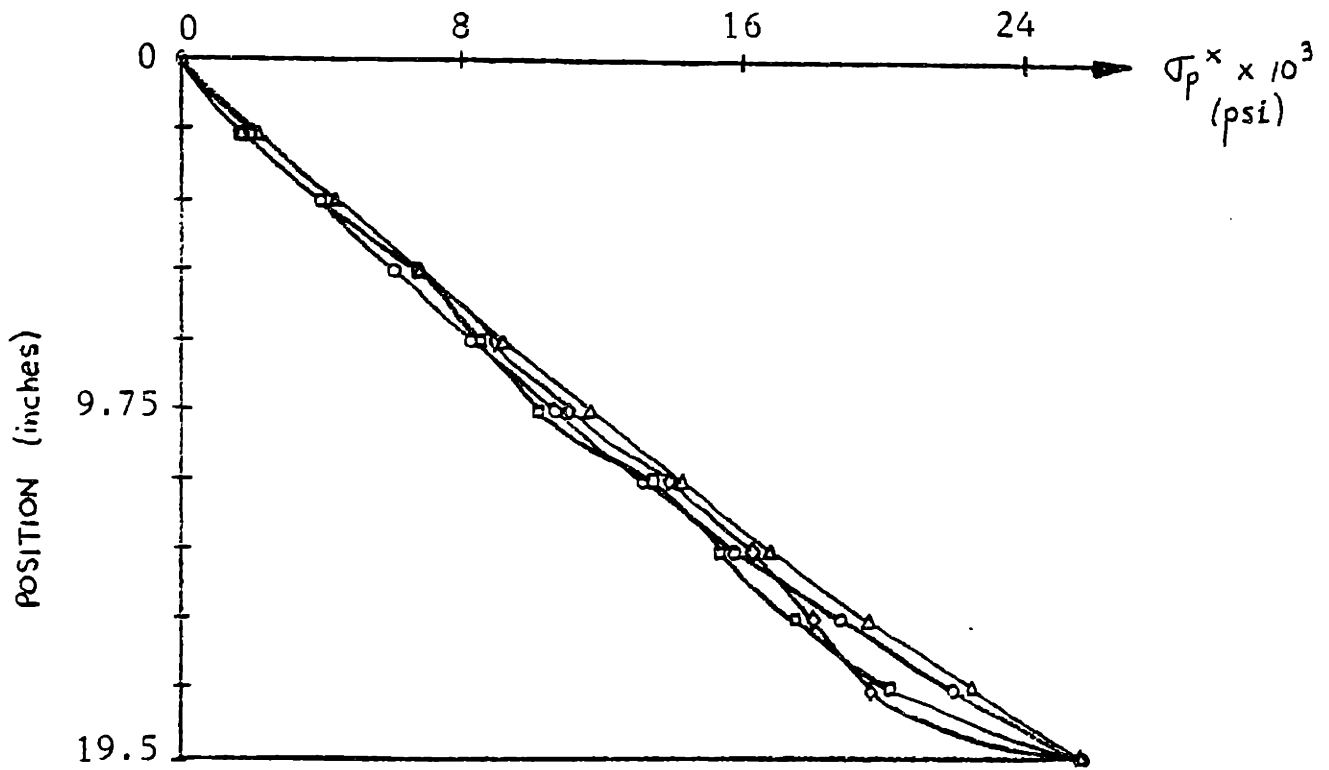
Figure 5.3. Longitudinal normal stress $\sigma_p{}^x$
in the pile
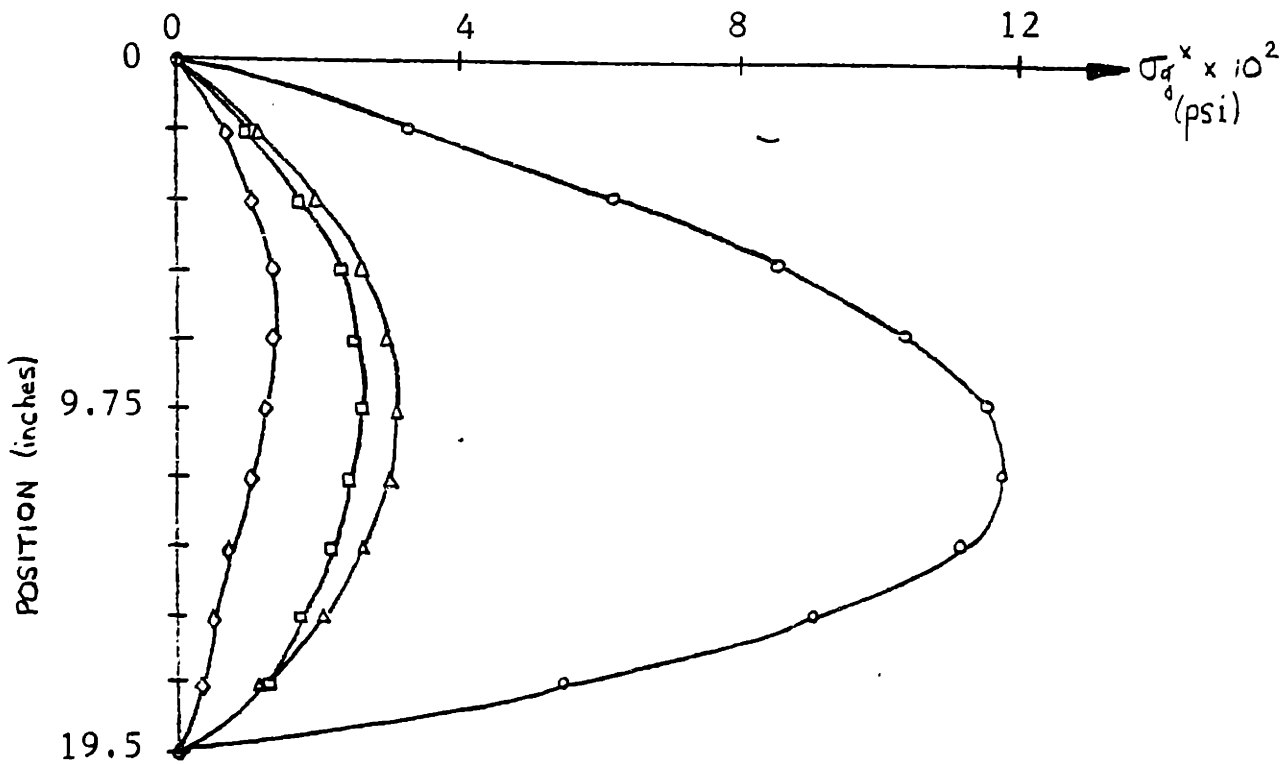
Figure 5.4. Longitudinal normal stress $\sigma_g{}^x$
in the grout

from $\sigma_g{}^x$ for the other two. Finite element results in the plastic range for slip equal to 0.033 in. are also included. The general form of the longitudinal normal stresses remains the same as the finite element results in the elastic range (slip equal to 0.030 in.) with an appropriate increase or decrease in the stresses in proportion to the average shear stress.

Figures 5.5, 5.6 and 5.7 give the longitudinal displacements $u_j{}^x$, $u_p{}^x$ and $u_g{}^x$, respectively, as a function of position.

Figure 5.5. exhibits good agreement between the three-dimensional and finite element models. However agreement with the one-dimensional model (with its exclusion of Poisson effects) is not as good. The same is true of Figures 5.6 and 5.7 where once again the finite element and three-dimensional models compare quite well, with only a slight deviation observed for $u_p{}^x$, whereas the general behavior of the one-dimensional results does not follow the seemingly correct trend of the other models.

As could be expected, the displacements in the jacket steel follow a quadratic form and differ more discernably in the upper part of the jacket nearer the load, while the displacements in the pile steel followed a similar quadratic form but with the increased displacement differential between subsequent positions along the pile occurring in the lower end of the pile where that load was
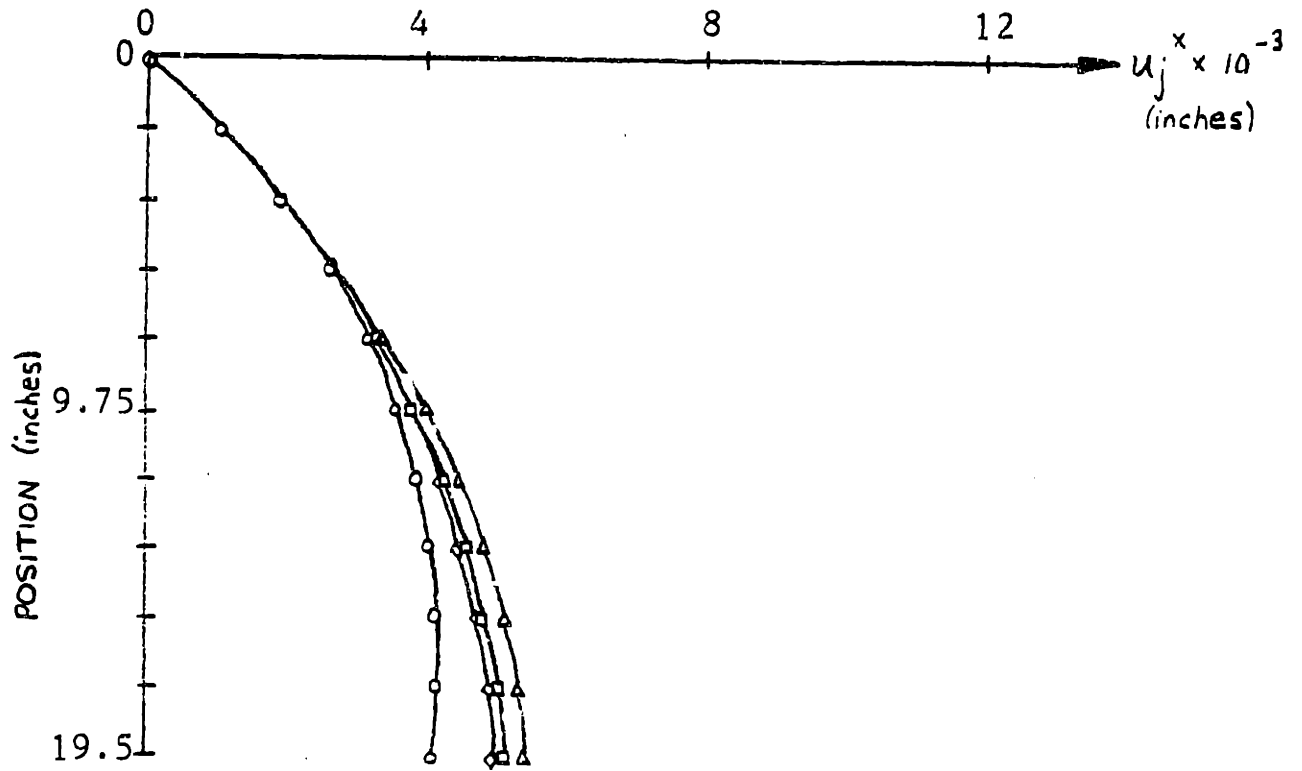
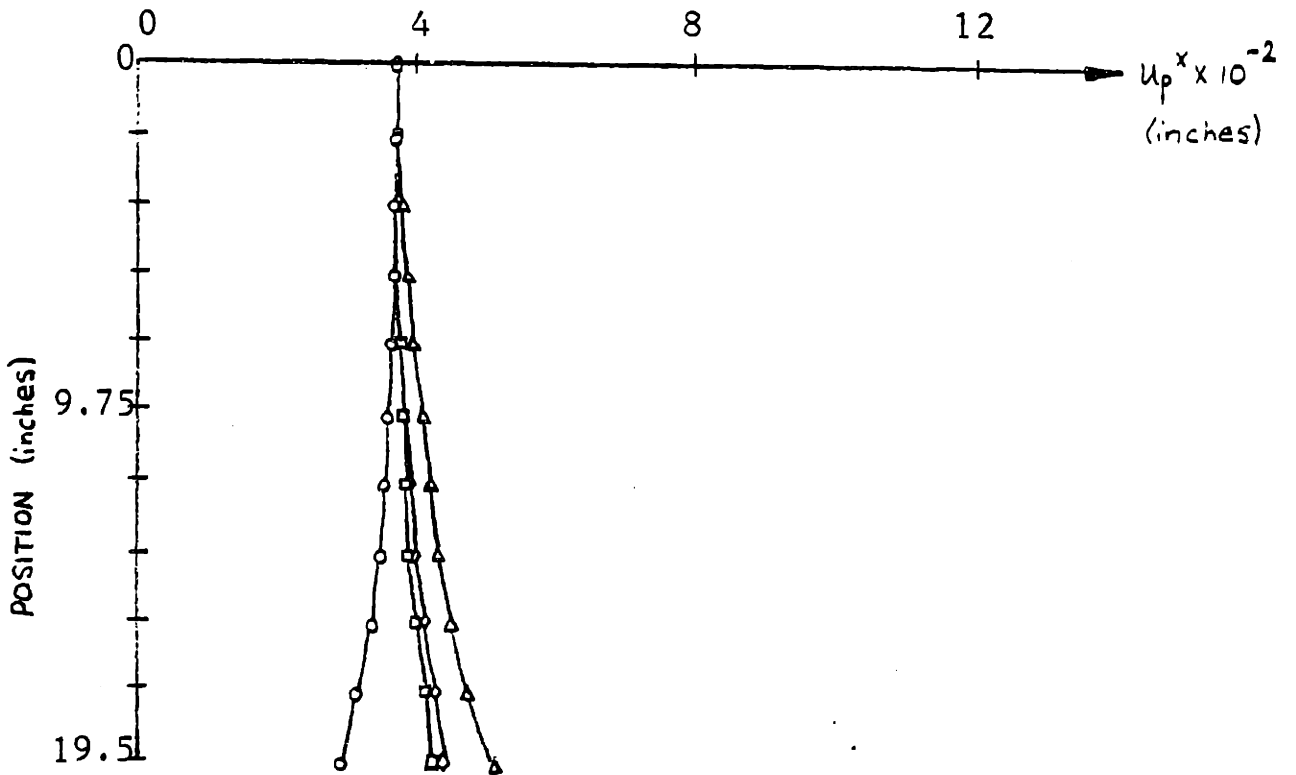Figure 5.5. Longitudinal displacement $u_j{}^x$ in the jacket

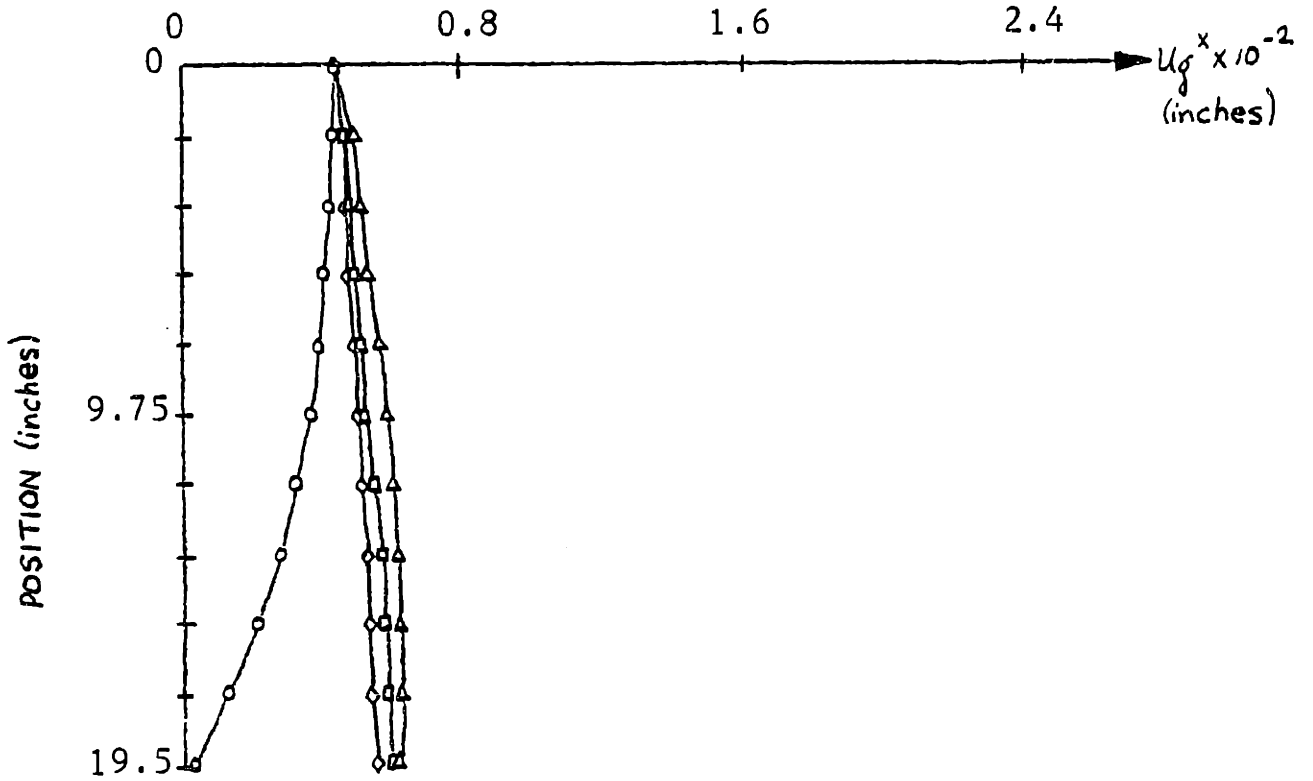Figure 5.6. Longitudinal displacement $u_p{}^x$ in the pile

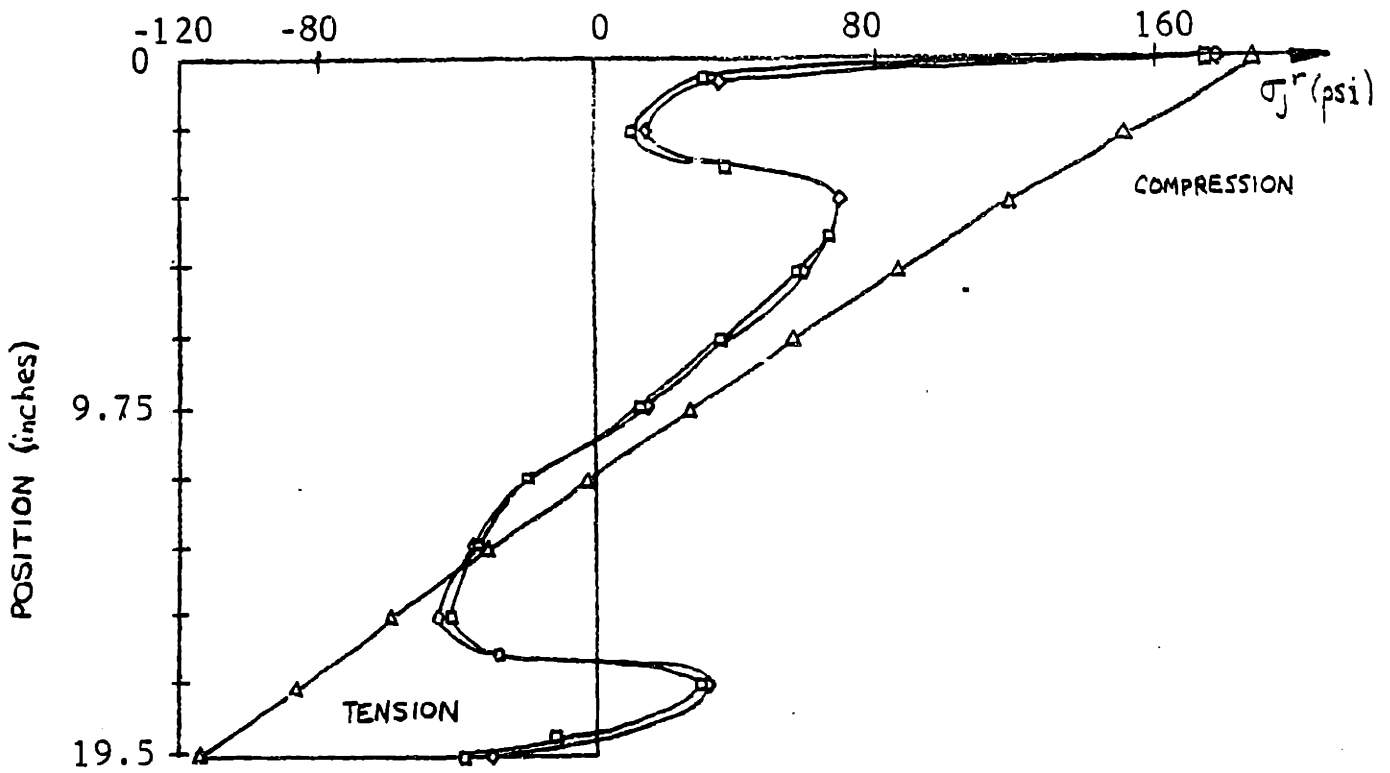Figure 5.7. Longitudinal displacement u_g^x
in the grout

Figure 5.8. Radial normal stress σ_j^r
at the jacket-grout interface

applied. The displacements in the grout are almost constant.

It is apparent that the total bond strength of the connection is a function of many parameters, one of which is the existence of friction between the steel and concrete. The frictional component is dependent on the normal forces between the two materials. Although the effect of friction on the bond strength is not considered herein, it is of interest to present the radial normal stresses at the interfaces. A more sophisticated model may include the effect of these stresses on the relation between shear stress and bond slip.

Figures 5.8 through 5.13 give plots of the radial normal stresses and the radial displacements for the three-dimensional and the finite element models. The three-dimensional model predicts an almost linear distribution of radial normal stresses. However the bending effects accounted for in the finite element analysis show an additional "sinusoidal" component especially near the two ends. At the jacket interface the finite element model gives an overall reduction in radial stress at the top and an overall increase in stress at the bottom. Similarly, effects show up at the pile interface.

The bending effects become less pronounced in the grout layer however. Figure 5.10 shows a slight rippling effect due to bending, with only slight deviations from
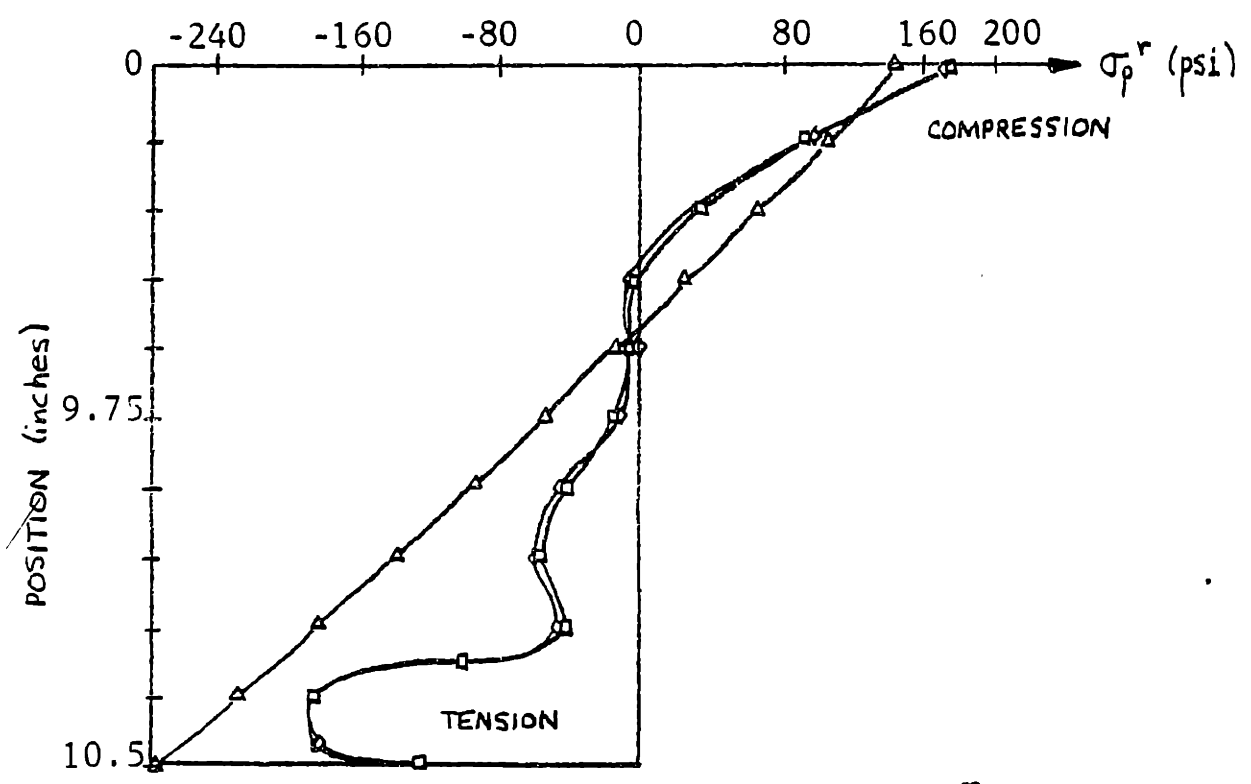
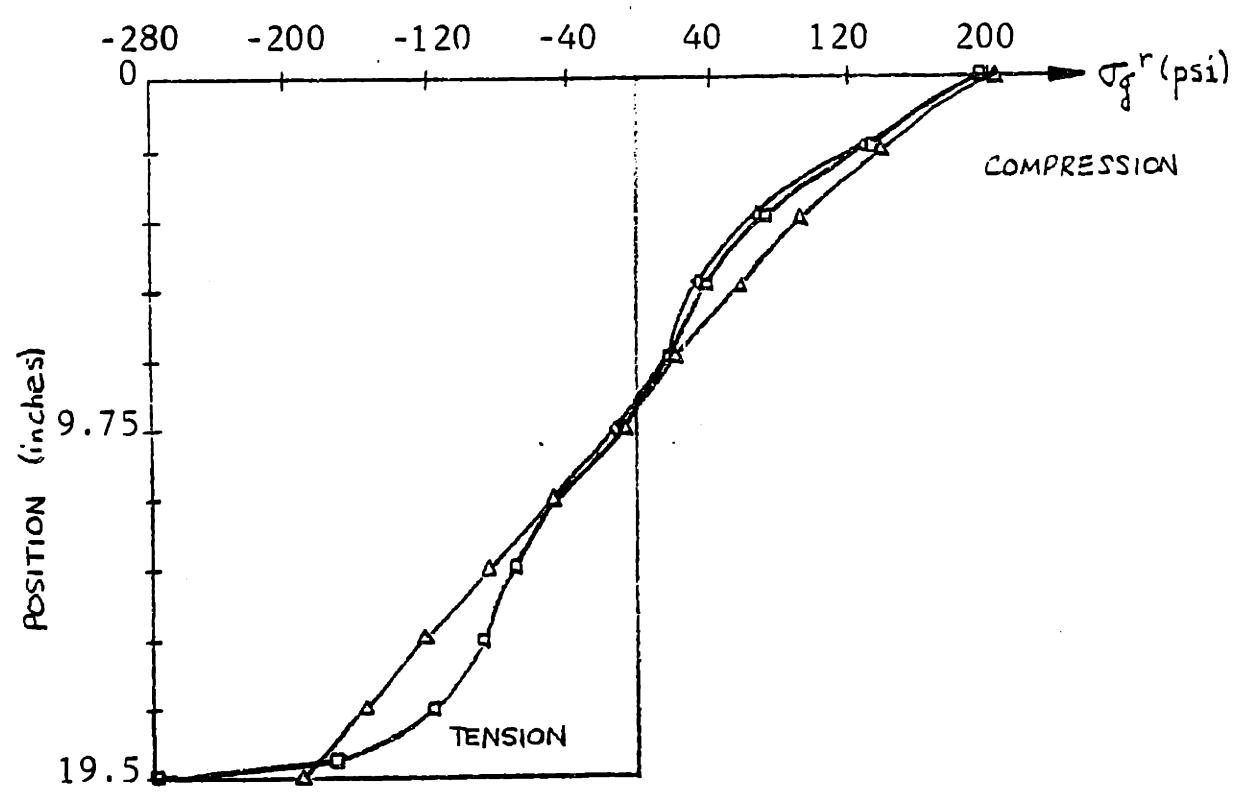Figure 5.9. Radial normal stress σ_p^r
at the pile-grout interface

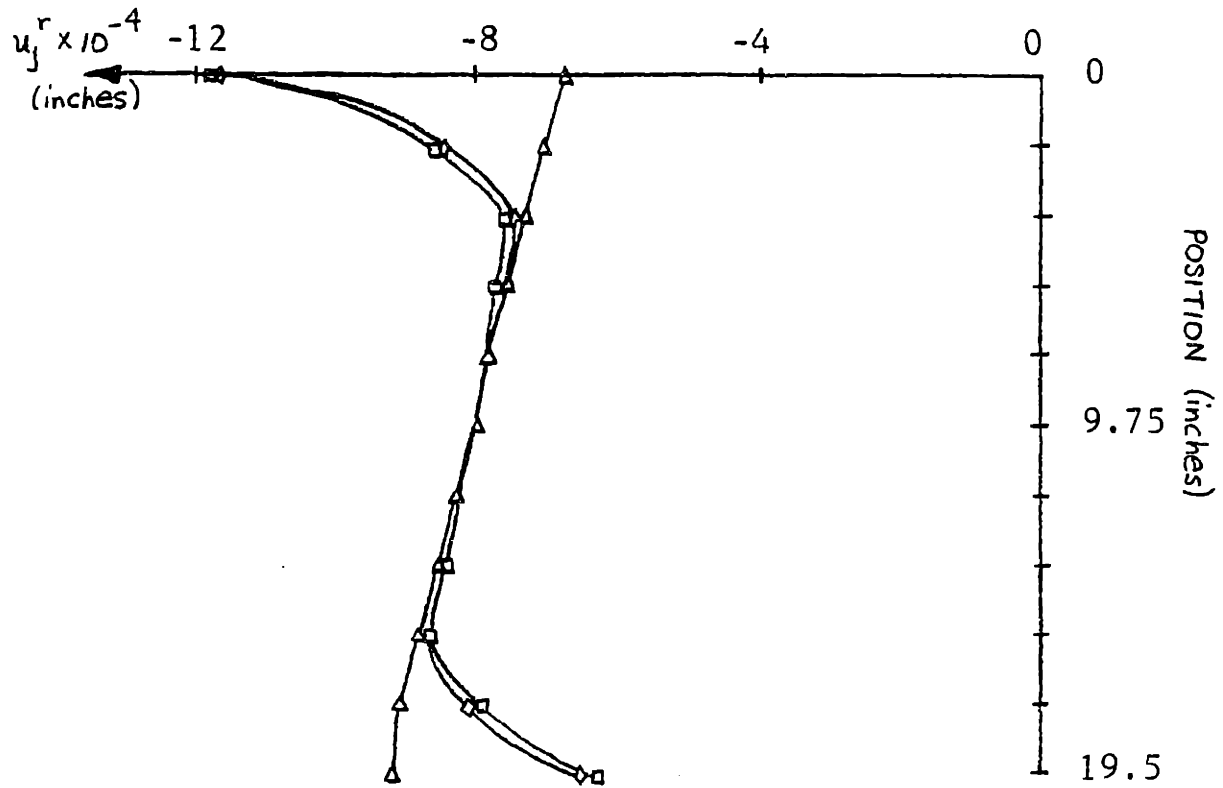Figure 5.10. Radial normal stress σ_g^r
in the grout

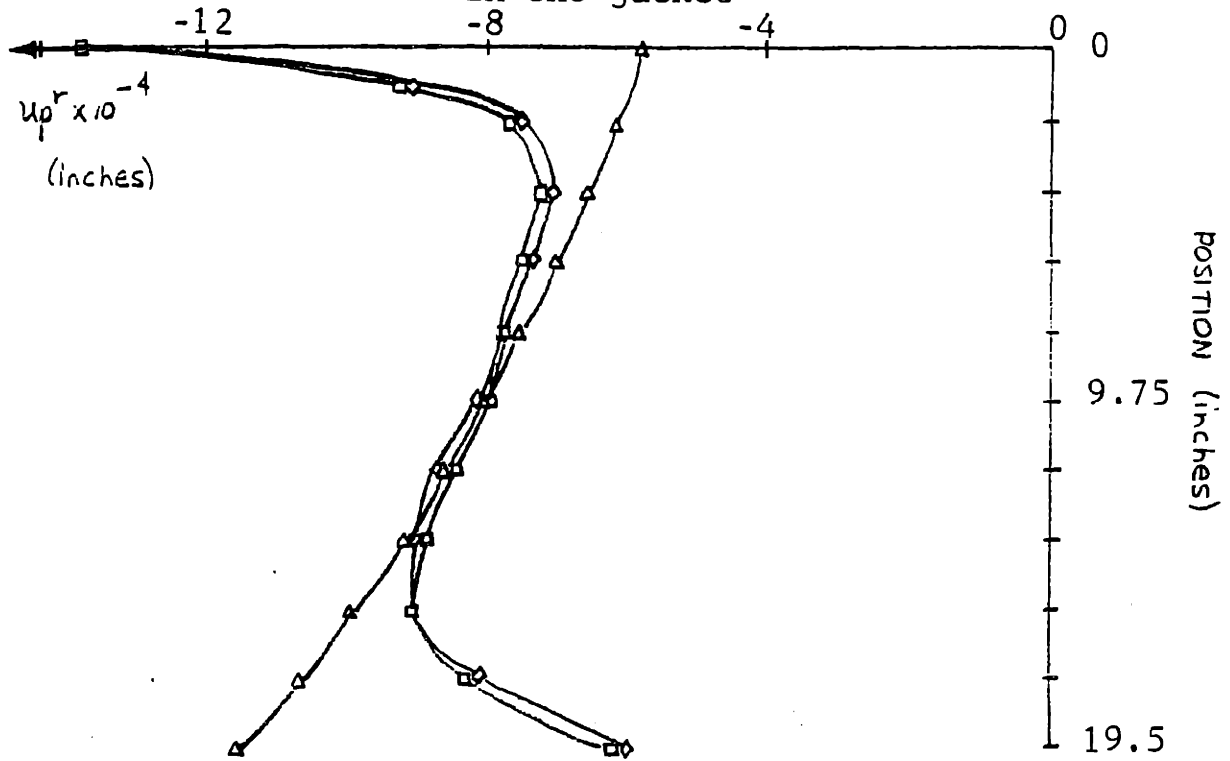Figure 5.11. Radial displacement $u_j{}^r$
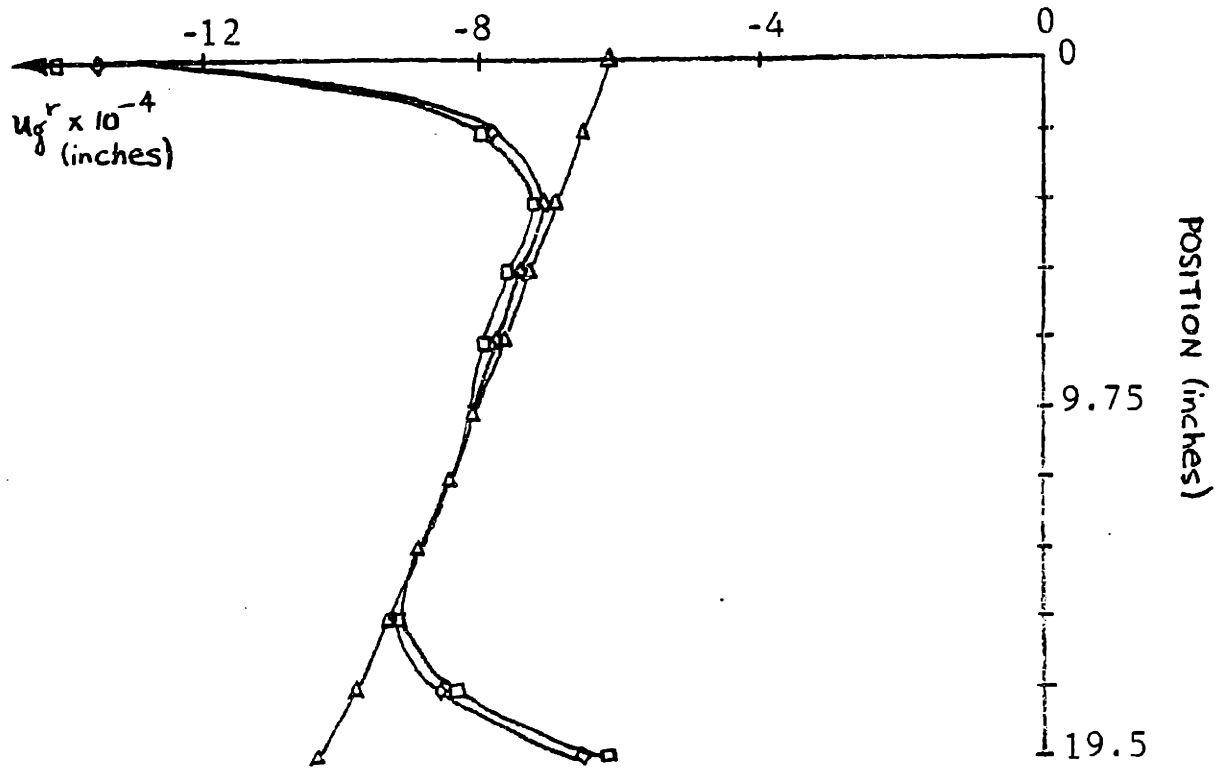in the jacket

Figure 5.12. Radial displacement $u_p{}^r$
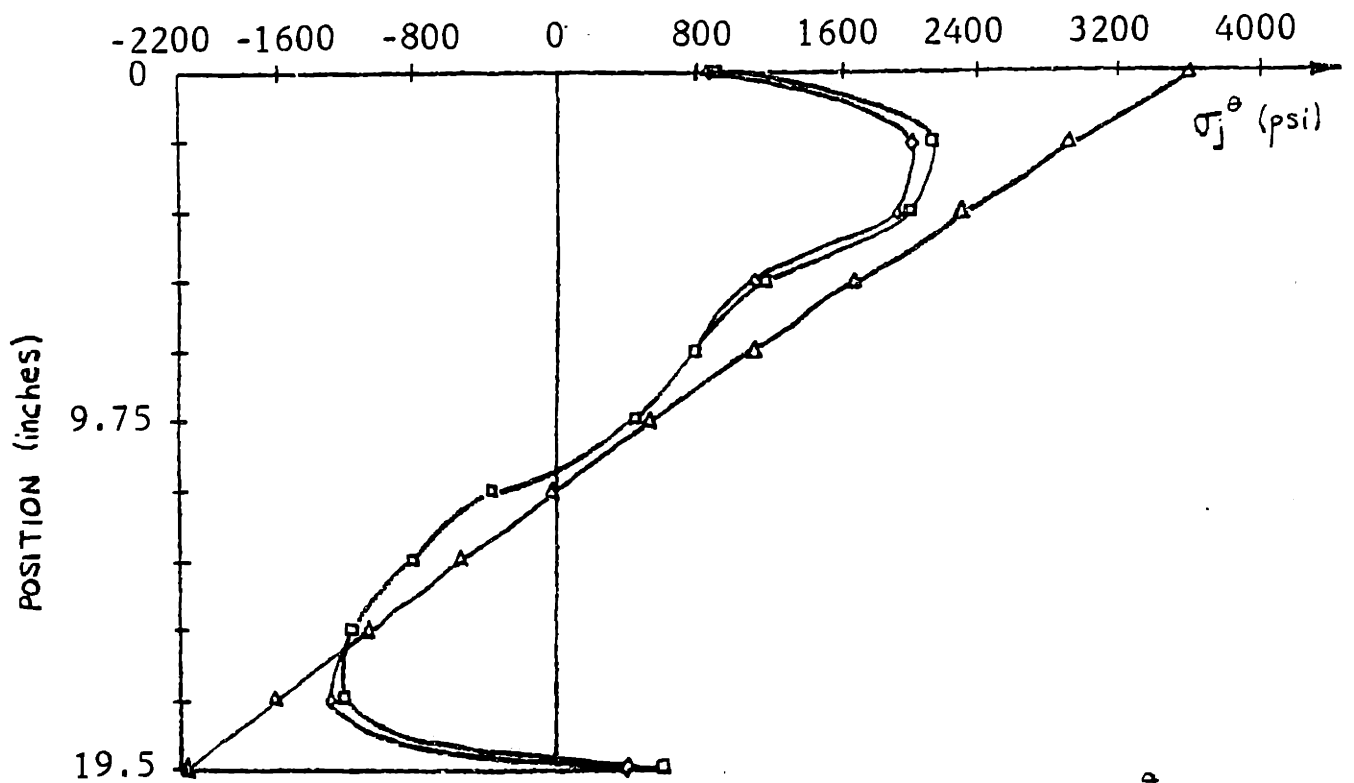in the pile

Figure 5.13. Radial displacement $u_g{}^r$
in the grout

Figure 5.14. Circumferential (hoop) stress $\sigma_j{}^\theta$
in the jacket

the linear distribution predicted by the three-dimensional model. Figures 5.8 through 5.10 show that, for the most part, the axial loading system introduces tensile radial stresses near the top and the opposite is true for the bottom part.

Figures 5.11 through 5.13 give plots of radial displacement of the jacket, the pile and the grout. Once again the bending effects are predominant at the upper and lower third of the connection while the middle portion compares well with the three-dimensional model.

Once again bending effects become apparent in the graphs of circumferential (hoop) stress in the jacket, pile and grout, presented in Figures 5.14 through 5.16. The circumferential stress in the jacket as predicted by the finite element model follows the three-dimensional model well with the additional of the "sinusoidal" bending effects. The stresses in the pile and grout differ substantially at the upper and lower ends of the connection implying that bending effects here are very pronounced.

It is important to note here that the non-linear behavior of the interface between the steel and the grout does not drastically affect the values of the longitudinal, radial or circumferential stresses or displacements. Finite element results in the elastic range only differ by a constant from those in the plastic range and this difference is in agreement with the difference in the
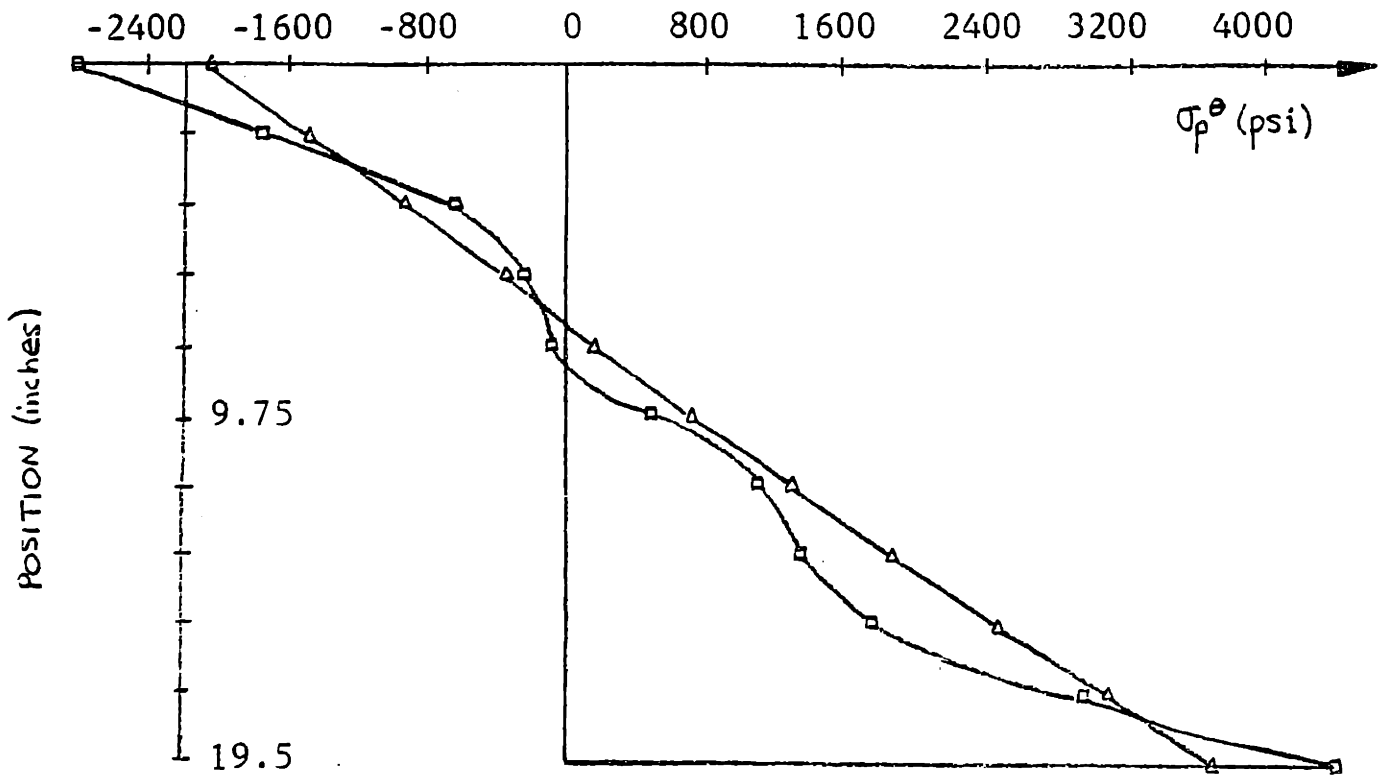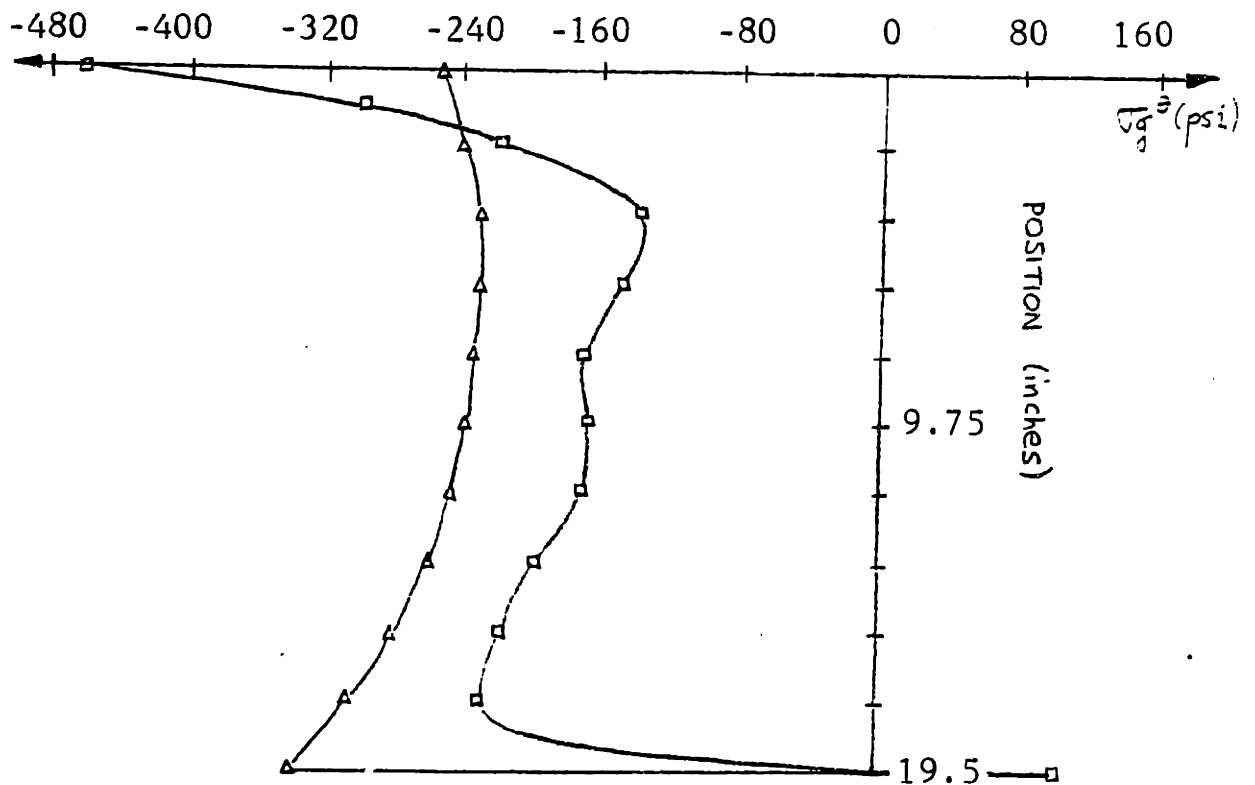
Figure 5.15.   Circumferential (hoop) stress σ_p^θ
in the pile

Figure 5.16.   Circumferential (hoop) stress σ_g^θ
in the grout

corresponding values of average shear stresses. The effect of the non-linearity of the interfaces becomes evident in the values of the shear stresses however.

Figures 5.17 through 5.19 show the plots of shear stresses in the jacket, pile and grout for the two analytical models and for three finite element models. The results of the one-dimensional model for shear stress along the jacket steel interface show poor correlation to the actual behavior. The three-dimensional and finite element models are in good agreement, with the exception of the jacket-grout interface. For the finite element model which includes the non-linearity of the interface and into the plastic range (slip equal to 0.043 in.), the distribution of the shear stress is similar and the values of shear are appropriately less.

The one-dimensional model provides better results for the pile-grout interface than for the jacket-grout one. The three-dimensional model and finite element model for slip equal to 0.030 in. provide better results. Since the average shear stress was calculated by using the contact area of the pile-grout interface, the average value of the stresses in Figure 5.18 must be equal to that value. The three-dimensional model corresponds to a slippage of 0.030 in. and to an average shear stress of 400 psi. This model predicts a distribution of shear stress ranging from 330 psi to 470 psi with an average value of approximately
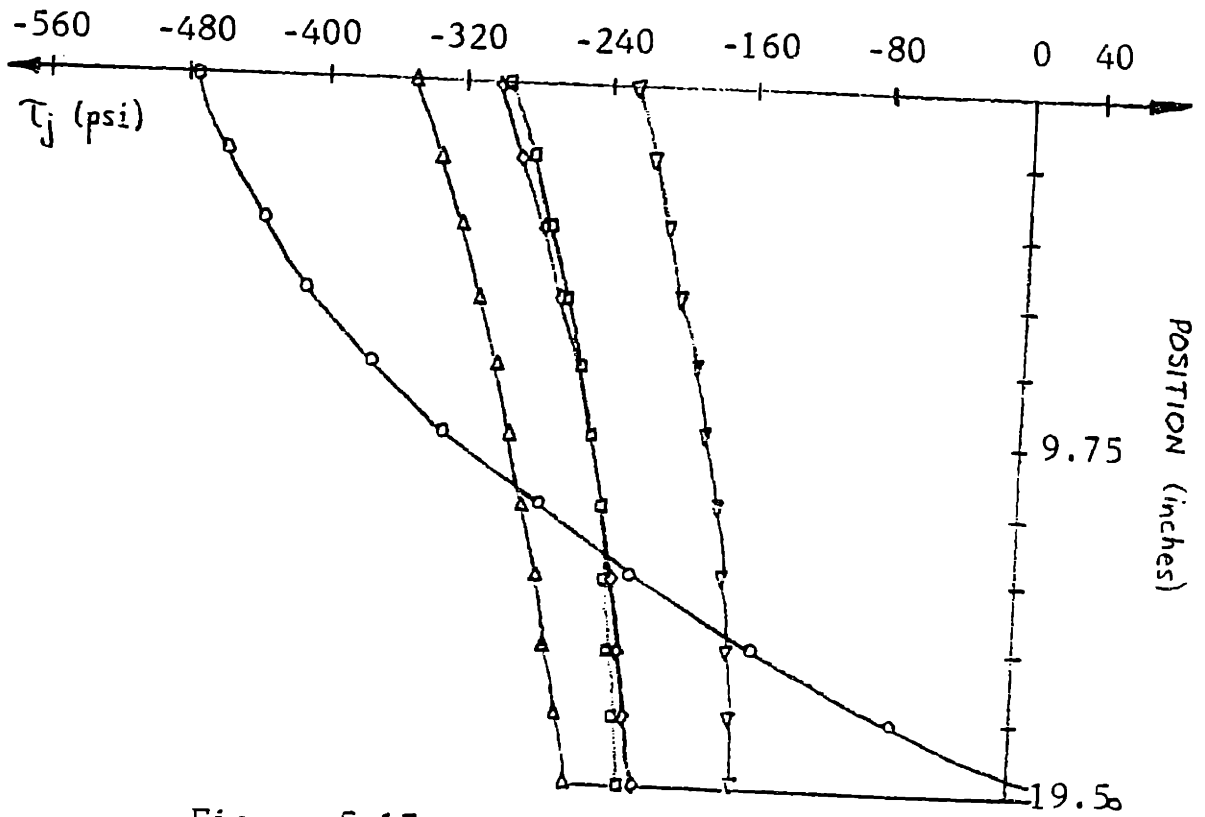
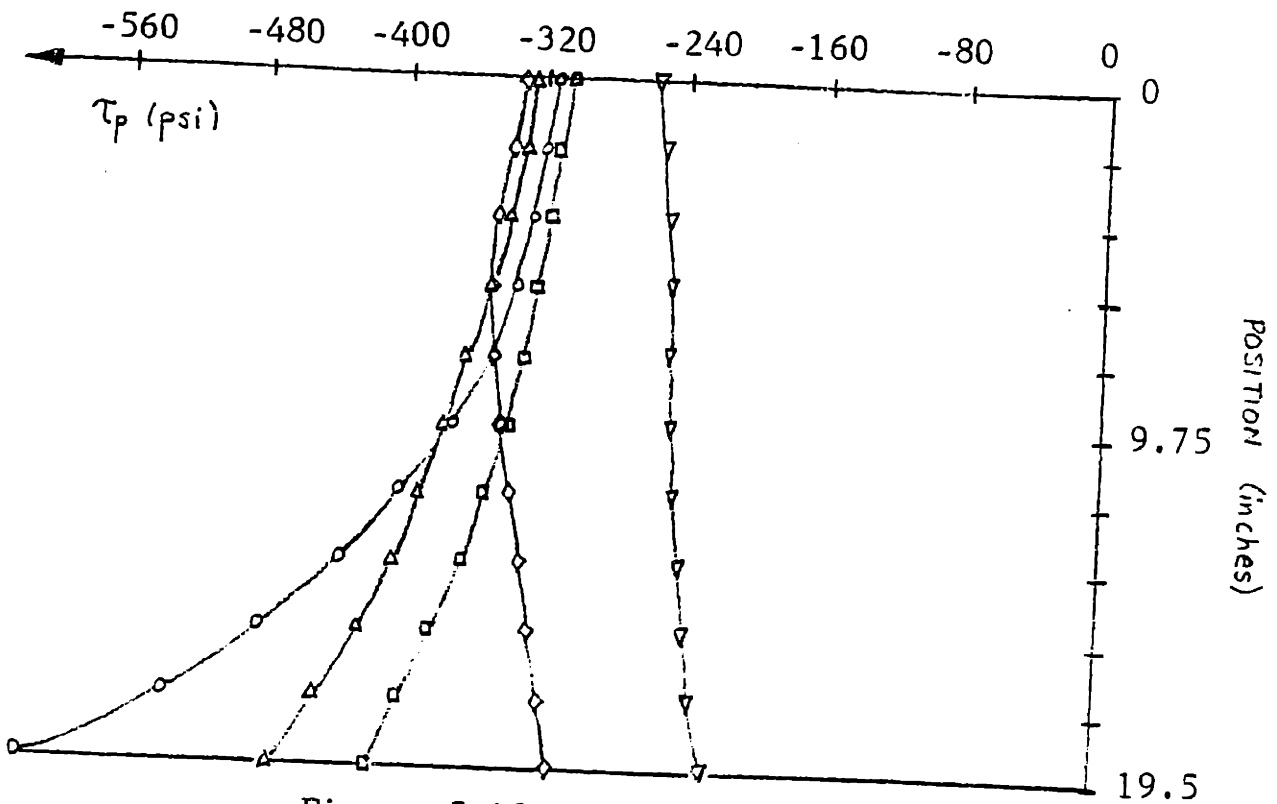Figure 5.17. Shear stress -- τ_j at the jacket-grout interface

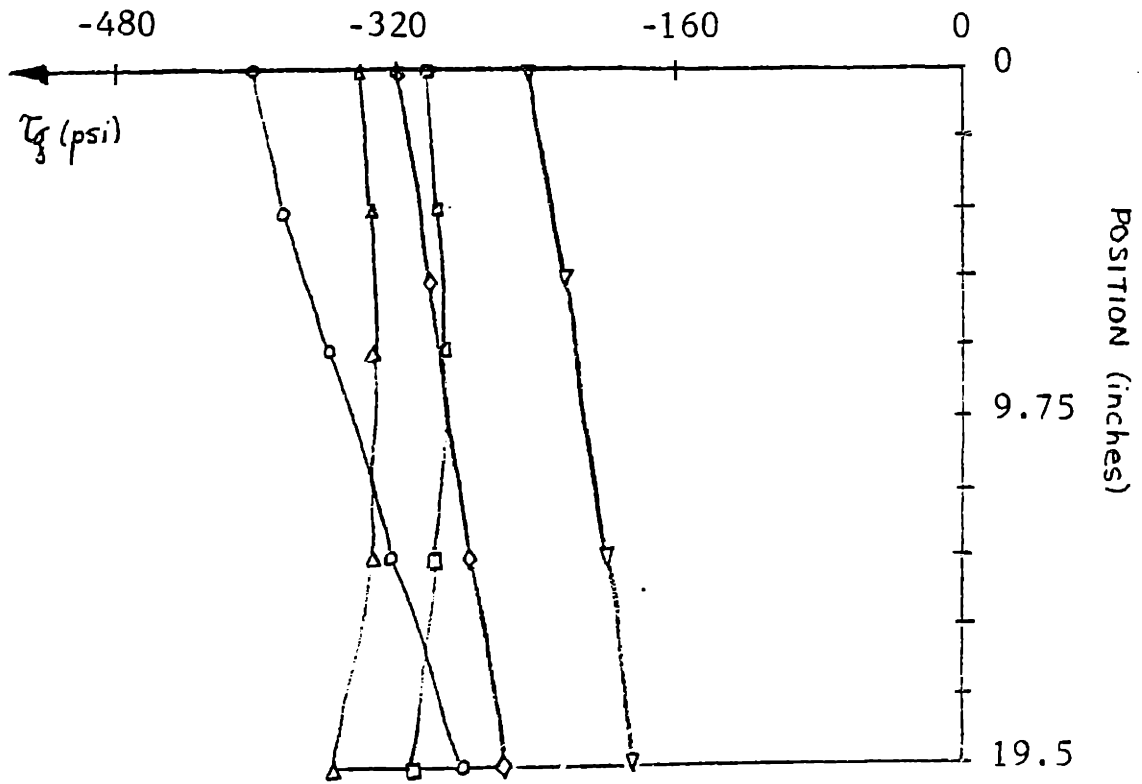Figure 5.18. Shear stress τ_p at the pile-grout interface

Figure 5.19.   Shear stress τ_g in the grout

400 psi. However the finite element model for slip equal
to 0.030 inch and τ_{avg} = 400 psi predicts a distribution
of stress ranging only from 310 psi to 410 psi with an
average value of approximately 360 psi. This value is
lower than the assumed overall average shear stress and
implies an inadequacy of the finite element model to pre-
dict accurately the shear stress distribution.

Even though the overall behavior of the connection
was non-linear for the inelastic finite element model
in Figure 5.17 (slip equal to 0.043 in.), the jacket-grout
interface was not in the plastic range because the shear
stresses there are much smaller than those along the grout-
pile interface where inelasticity occurs. As a result,
the distribution of shear stress along the jacket inter-
face follows the same trend as the elastic results.

The results of the finite element model for slip
equal to 0.033 in. and τ_{avg} = 396 psi (Figure 5.18)
show the effects of the non-linearity of the pile-grout
interface on the shear stress here. Within the top 4.000
in., the interface remains elastic. Beyond that point
the plastic behavior begins to govern and a gradual de-
crease in shear stress becomes evident. For slip equal
to 0.043 in. and τ_{avg} = 300 psi the finite element re-
sults show that the entire interface is in the plastic
range, and the shape of the shear stress distribution is
different from that in the elastic range. The difference

is more noticeable near the bottom of the connection.

Figure 5.19 gives the plot of shear stress in the grout. The one-dimensional model does not adequately predict the behavior of the grouted pile connection while the three-dimensional model appears valid in the elastic range. The finite element model predicts elastic shear stresses which are less than those implied by the external load but the distribution of which agrees with the three-dimensional model. In the plastic range, the finite element models show a change in the distribution of the shear stress.

Figures 5.20 through 5.22 show the plots of shear stresses in the jacket, pile and grout when the interface between the steel and grout is assumed very stiff or ignored all together. As can be seen in these graphs, a rough, stiff interface leads to a non-uniform distribution of shear stress along the connection with peaks near the ends and small values at the center. In this case, the tendency to describe the strength of the connection by an equivalent average shear stress becomes invalid. This study shows that such a simplification which ignores the stiffness of the steel-grout interface incurs significant error and fails to accurately predict the behavior of grouted pile connections.
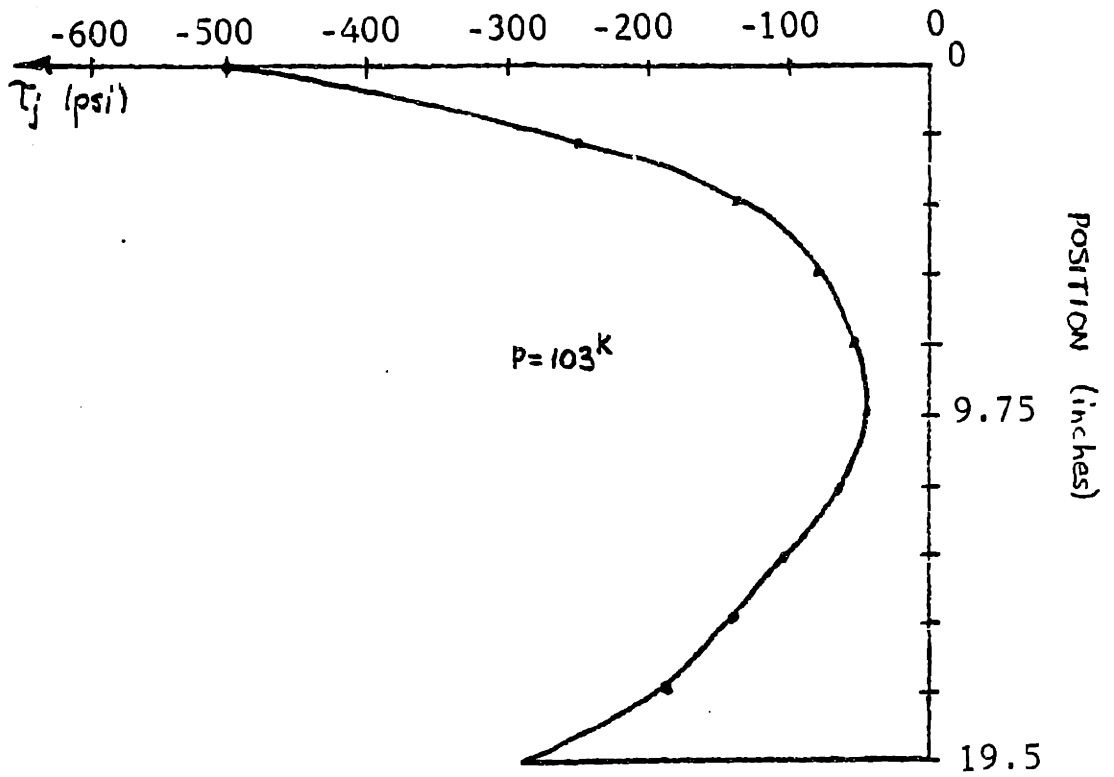
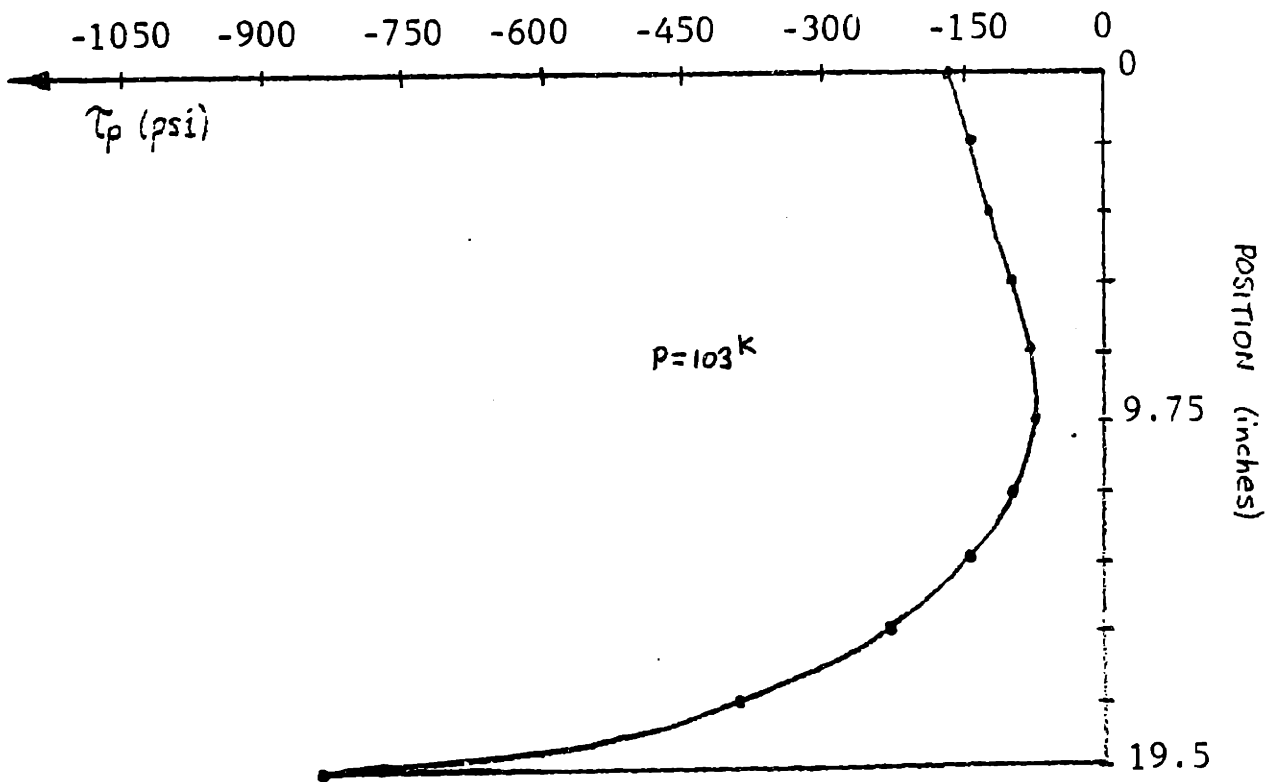Figure 5.20. Shear stress τ_j for a very stiff jacket-grout interface

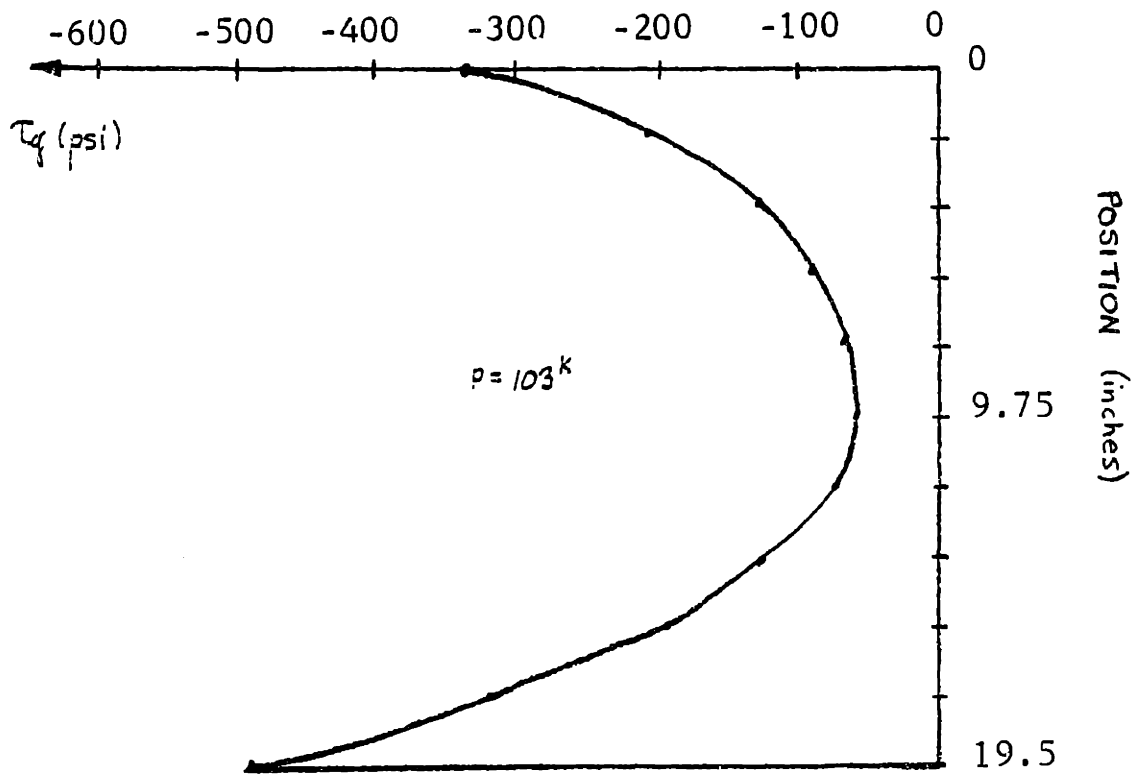Figure 5.21. Shear stress τ_p for a very stiff pile-grout interface

Figure 5.22.   Shear stress τg for a very
stiff steel-grout interface

CHAPTER 6: CONCLUSIONS AND DESIGN RECOMMENDATIONS

In this thesis, the behavior of grouted pile connections has been studied with emphasis on defining the principal parameters which affect strength and on establishing mathematical models which include the effects of these parameters and predict the behavior of the connection.

The major conclusions of this study are:

1) The ultimate bond strength of grouted connections depends mainly on the following two characteristics of the interface between steel and grout: on the stiffness (which determines the distribution of shear stress along the connection) and on the local bond strength of the interface. A rough, stiff interface leads to a nonuniform distribution of shear stress along the connection, with peaks near the ends and a small value at the center. On the contrary, a smooth, flexible interface leads to uniform distribution of shear stress along the connection.

2) Poisson effects on the behavior of grouted pile connections can be significant due to the fact that the three-dimensional stress state can be an important parameter in determining the amount of friction bond since the latter is dependent on the normal stresses on the interfaces. The three-dimensional model presented herein can be easily modified to include the dependence of bond on normal stress.

3) No significant bending effects are present in the longitudinal stresses but become more significant in the radial and circumferential stresses. It is considered, however, that the effect of bending on the strength of the connection is negligible. This justifies the use of a three-dimensional model which includes Poisson effects but ignores bending.

4) The current practice of describing the strength of axially loaded grouted connections in terms of an equivalent average bond stress appears

justified for realistic stiffnesses of the steel-grout interfaces.

5) The normal stresses and displacements do not change appreciably when the behavior of the steel-grout interface becomes plastic. More importantly, the shape of the shear stress distribution changes only slightly. Therefore the equivalent average bond strength is a valid description of the strength of the connection under both elastic and plastic conditions of the steel-grout interfaces.

6) A three-dimensional analytical model was developed which adequately predicts the behavior of grouted pile connections. This model accounts for cylindrical geometry, all important material properties of both steel layers and of the grout, for the stiffness of the steel-grout interface and for Poisson effects.

7) The post-ultimate slip-deformations along the connection can be predicted only by the non-linear finite element model.

REFERENCES

Bathe, Klaus-Jurgen; "ADINA: A Finite Element Program
     for Automatic Dynamic Incremental Nonlinear Analysis",
     Report 82448-1, Massachusetts Institute of Technolo-
     gy, September 1975.

Billington, Colin J. and Gael, H. G. Lewis; "The Strength
     of Large Diameter Grouted Connections", Paper #3083 -
     Offshore Technology Conference, May 1978.

Kraft, L. M., Jr. and Lyons, C. G.; "State of the Art:
     Ultimate Axial Capacity of Grouted Piles", Paper
     #2081 - Offshore Technology Conference, May 1974.

Nilson, A.; "Internal Measurements of Bond Slip", ACI
     Journal, July 1972.

Ostroot, G. Warren; "The Bond Strength of Offshore Plat-
     form Grouts;, Chemical Research and Development,
     Report No. C43-A001-78, April 11, 1978.

Sherman, Donald R.; "Pullout Bond Strength of Concrete
     in a Steel Pipe", Paper #2305 - Offshore Technology
     Conference, May 1975.